Towards accelerated thermoelectric materials and process discovery

Jose Recatala-Gomez[‡⊥]#, Ady Suwardi[‡]#, Iris Nandhakumar[⊥]*, Anas Abutaha [‡]*, Kedar Hippalgaonkar [§‡]*

[§] School of Material Science and Engineering, Nanyang Technological University, Singapore 639798.
[‡] Institute of Materials Research and Engineering, #08-03, 2 Fusionopolis Way, Agency for Science, Technology and Research, Singapore 138634.
[⊥] Department of Chemistry, University of Southampton, University Road, Highfield, Southampton SO17 1BJ, United Kingdom.
# equal contribution

* corresponding authors: kedar@ntu.edu.sg; iris@soton.ac.uk; anas@imre.a-star.edu.sg

Abstract

Thermoelectric materials have the ability to convert heat energy to electrical power and vice versa. While the thermodynamic upper limit is defined by the Carnot efficiency, the material figure of merit, ZT is far from this theoretical limit, typically limited by a complex interplay of non-equilibrium charge and phonon scattering. Materials innovation is a slow, arduous process due to the complex correlations between crystal structure, microstructure engineering and thermoelectric properties. Many physical concepts and materials have been unearthed in this path to discovery, supported ably by innovations in technology over many decades, revealing important material and transport descriptors. In this review, we look back at some case studies of inorganic thermoelectric materials employing a birds-eye view of complementary advancements in scientific concepts and technological advancements and conclude that most high values of zT have emerged from new scientific ideas fueled by moderately mature technologies. Based on this conclusion, we then propose that the recent emergence of data-driven approaches and high throughput experiments, encompassing synthesis as well as characterization, with machine learning guided inverse design is perfectly suited to provide an accelerated pathway towards the discovery of next-generation thermoelectric materials, potentially providing a feasible alternative source of energy for a sustainable future.

Keywords: thermoelectric, accelerated discovery, high throughput experiments, high throughput characterization, data-driven, machine learning

Introduction

Thermoelectrics (TE) is a field at the forefront of materials chemistry, novel physics and engineering.[1] This is because development of new thermoelectric technologies not only requires deep understanding of how materials are put together, but also requires in-depth knowledge of out-of-equilibrium transport phenomena: of how heat and charge transport and scattering occurs, as well as engineering of devices. The efficiency of heat-to-power (and vice versa) conversion of a thermoelectric material is gauged by the figure of merit zT at a thermodynamic temperature T, defined as $S^2\sigma T/\kappa$, where S is Seebeck coefficient representing how much entropy is carried by a majority carrier (typically in a semiconducting material), σ is the electrical conductivity and κ is the thermal conductivity.[2] The thermal conductivity has two components, that which is carried by the charge carriers (electronic thermal conductivity, κ_e) and lattice vibrations or phonons (lattice thermal conductivity, κ_l).[3] A zT value of 4 or more can be competitive with existing energy generation and/or cooling technologies, providing a viable sustainable energy alternative.[4] The technology is immensely attractive as it involves non-moving parts and solid-state devices.

Innovation in thermoelectrics is limited by discovery of new materials and even though device architectures have been considered and studied in some details[5–7], the major challenge is to design a high performance TE material – this involves a complex process of identifying the key material and transport descriptors that can be used to predict a new thermoelectric material. For instance, an ideal thermoelectric is a 'phonon glass electron crystal' where charges can flow unimpeded, while a large temperature gradient can be maintained across the material.[8] However, the band structure of the material is of paramount importance as well, since normal metals are not good at maintaining a thermal voltage (a small Seebeck coefficient), due to the small asymmetry of the density of states at the fermi level, typically since the Fermi level is in the middle of the band.[9] Hence, degenerately doped semiconductor crystals are favorable as thermoelectric materials. Looking at the constituent atomic level, those that have large masses and a large number of atoms in the unit cell result in large valley degeneracies in a complex electronic band structure,[10] while at the same time, massive atoms manifest as sluggish acoustic phonons, thereby improving thermoelectric performance.[11]

In addition to material descriptors, transport descriptors are also critically important. Using the Landauer formalism, thermoelectric transport can be understood well as a linear response function to electric and thermal fields.[12] Hence, the scattering of charges and phonons, when out of their respective ground state distribution functions is vital for energy conversion performance.[13] For instance, low effective mass charges are favorable to obtain high mobility which translates to high electronic conductivity. However, this is counter-productive for Seebeck, which requires a large Density of States effective mass (and shallower bands, therefore providing large asymmetry around the Fermi Level). Hence, a balance between large and small effective masses is necessary, typically achieved through a complex bandstructure (Fermi surface complexity).[14] Large valley degeneracy and high symmetry crystal structures provide for long scattering times, therefore increasing the carrier mobility, and through other valleys (in an energy window within a few ~k_BT) in different parts of the Brillouin Zone, a large Seebeck can simultaneously be obtained. However, intervalley scattering can reduce the mobility and decrease the electrical conductivity.[15] Therefore, carefully choosing materials that have favorable charge scattering rules to enhance relaxation times, while still providing high Seebeck is an open challenge. Material systems that are binary, ternary and quaternary and beyond can produce optical phonon modes with low group velocity, therefore systematically reducing thermal conductivity; in addition, a complex band structure can provide a playground for rich physics to enhance thermoelectric properties. However, beyond ground state bandstructure, predicting phase stability of such compounds is a formidable challenge and hence such materials have largely remained unexplored. First principles calculations have aided discovery in leaps and bounds, with databases such as Materials Project[16], AFLOWLIB[17], Citrination[18], Materials Data Facility (MDF)[19], Materials Platform for Data Science (MPDS)[20] ,Open Quantum Materials Database (OQMD)[21] and PoLyInfo[22] among many others, providing insightful information about material band structures. In the context of thermoelectrics, accuracy of information about complex materials, especially made from d- and f-block metals is still lacking – especially in the case of electron correlations. In addition, dopability of material systems to optimize carrier concentration levels to maximize power factor ($S^2\sigma$) and eventually zT is a difficult task that goes beyond mere material and defect-level predictions towards process selection and optimization.

There have been substantial improvements in material zT values over the last 70 years in chalcogenides[23], layered compounds[24,25], half-heuslers[26], skutterudites[27] as well as oxide-based materials[28], with advancements coming in the form of new physical concepts[29] as well as novel

materials chemistry[30] and process innovation.[31] However, given the complexity of the design space, the pace of innovation has been slow. We now have new tools available to materials chemists and physicists in the form of machine learning, data science, high-performance computing and robotics/automation driven high-throughput experiments. Therefore, our review is aimed at looking back historically at developments in the field and learning how innovation can be sped up with such new tools.

Evolution of TE materials performance

We look at these developments by categorizing using two key principles: improvements in physical and chemical understanding, as well as improvements in technology and experimental synthesis capabilities. The key question that we would like to address is whether the evolution towards high zT has been enabled primarily by

A. an advancement in technologies related to materials processing and synthesis? or
B. new physics and/or new materials systems?

This is an important question to answer, since it can inform us about the ability to wield these new tools in the right parameter space. Machine learning and data science have the ability to provide a large set of generative models that link inputs to outputs, and if parametrized properly, can be used for inverse design. Hence, to leverage on high-dimensional optimization and learning, it is important to define the input parameter manifold, which will have to be posed differently for the two different approaches above. For instance, if the target is discovery of new materials, vectorizing known materials with unique fingerprints accounting for atomic information, bond parameters, crystal structure etc is key: the first step for a machine learning algorithm is to learn from labeled, and hopefully vast data. Tools to gather such data have started to become available, for instance Matminer, an open source Python library that provides easy access and data manipulation do four of the most widespread materials databases (Materials Project[16], Citrination[18], Materials Data Facility (MDF)[19] and Materials Platform for Data Science (MPDS)[20]). Matminer's core functions are mostly taken from another Python library, the Python Materials Genomics (pymatgen)[32], which makes matminer a very powerful tool for both data mining and additional data processing and analysis. Another emergent and increasingly popular tool for the mining of underlying data is Natural Language Processing techniques (NLP). Here, words are directly correlated to high-dimensional vectors (embeddings) in a way that the syntactic and semantic relationships that the words embody are

preserved. For instance, the word "*chalcogenide*" could be preferentially associated to *"thermoelectrics"* as opposed to "*ferroelectrics"*. The most successful case of the application of NLP techniques to materials science has been carried out by Tshitoyan and collaborators. By collecting, processing and deploying unsupervised ML techniques on almost 3.3 million scientific abstracts, they could capture complex underlying concepts, such as structure-property relationships in the materials.[33] Another crucial resource in data mining is the well-established Inorganic Crystal Structure Database (ICSD), which compiles experimental data on every crystal structure ever experimentally characterized.[34] Since a crystal structure contains fundamental high quality data, such as the space group of a material, the Wyckoff positions of the atoms in the unit cell and the crystallographic parameters amongst others, having the ICSD data provides an important link to experimental verification.

On the other hand, if the target is to optimize the phase, microstructure and doping once the material is identified, the data frame needs to be thought about differently. Obtaining the right stoichiometry and doping level to achieve optimized thermoelectric performance is a trial-and-error process that involves navigating experimental parameters depending on the method being used, where the input-output parameter space can be defined as a set of experimental conditions and the output, for instance, being the right XRD spectrum of the material synthesized and the correct doping level. Recent work has catalogued a database of experimentally synthesized thermoelectric materials, with an easy-to-access API (tedesignlab.com)[35–37], but much remains to be done. Text-based mining of recipes for materials synthesis provides an interesting alternative to manually curating data and has recently garnered interest, although this has not been applied to the specific case of thermoelectrics yet.[38] Therefore, innovation can be a complex and tortuous path, progressing through identification of a new material followed by developing a synthesis process, driven by a knowledge of materials and transport descriptors.

The two driving forces for the discovery of new materials are the scientific principles behind the high performance and the synthesis and characterization techniques at one's disposal. For instance, larger zT values started to be reported with the development of the laser flash technique, thus enabling the accurate measurement of the thermal conductivity. In the scientific side of the story, larger zT values were reported by using band convergence as the necessary strategy for optimized electronic power factor.[10] Herein, we scrutinized the technological developments and scientific advances that enabled high zT in traditional and emerging TE materials. We established a rating system ranging from *'novel'* to *'mature'* in both categories.

While individual values are only a guide, the trends they exhibit are illuminating. Conceptually unique physical advances are rated higher in our scale whilst old concepts are rated as mature. For instance, alloying to reduce the lattice thermal conductivity[39] has a low rating while a Peierls instability as source of strong electron-phonon coupling is rated high.[40] Technological developments are rated according to their originality. In this case, established techniques such as the temperature-gradient methods for single-crystal synthesis[41] are rated low while high-throughput methods, such high-throughput bulk synthesis are highly rated.[42] The reasoning behind these choices is obvious: novel ideas will deepen the knowledge of the materials and thus will lead to new, more efficient strategies for the enhancement of the performance. The technological advances are rated in order to enable the prediction of how the new paradigm in automation, leading to the idea of a self-driven lab, support the discovery of new materials by reducing the time between discovery and commercialization as well as the overall cost.[43]

Building upon this analysis, we now define the guidelines that the innovation path in TE materials may follow. To do so, we first discuss the material and transport descriptors that define good thermoelectrics in detail. Then, we revisit the historical evolution of some chalcogen-based cornerstone materials for TE applications (hereinafter called “Case Studies”) and analyze the depth of knowledge and the technological progress that led to their success, therefore providing a perspective to future researchers on where the key bottlenecks lie.

In order to accelerate thermoelectrics materials development, a combination of data generation, machine learning, high-throughput experimentation (including synthesis and characterization) and high-performance computing needs to be employed. We find that the path of innovation in TE materials has typically been driven by novel, unexplored physical and chemical phenomena and executed *via* deployment of mature technological processes.

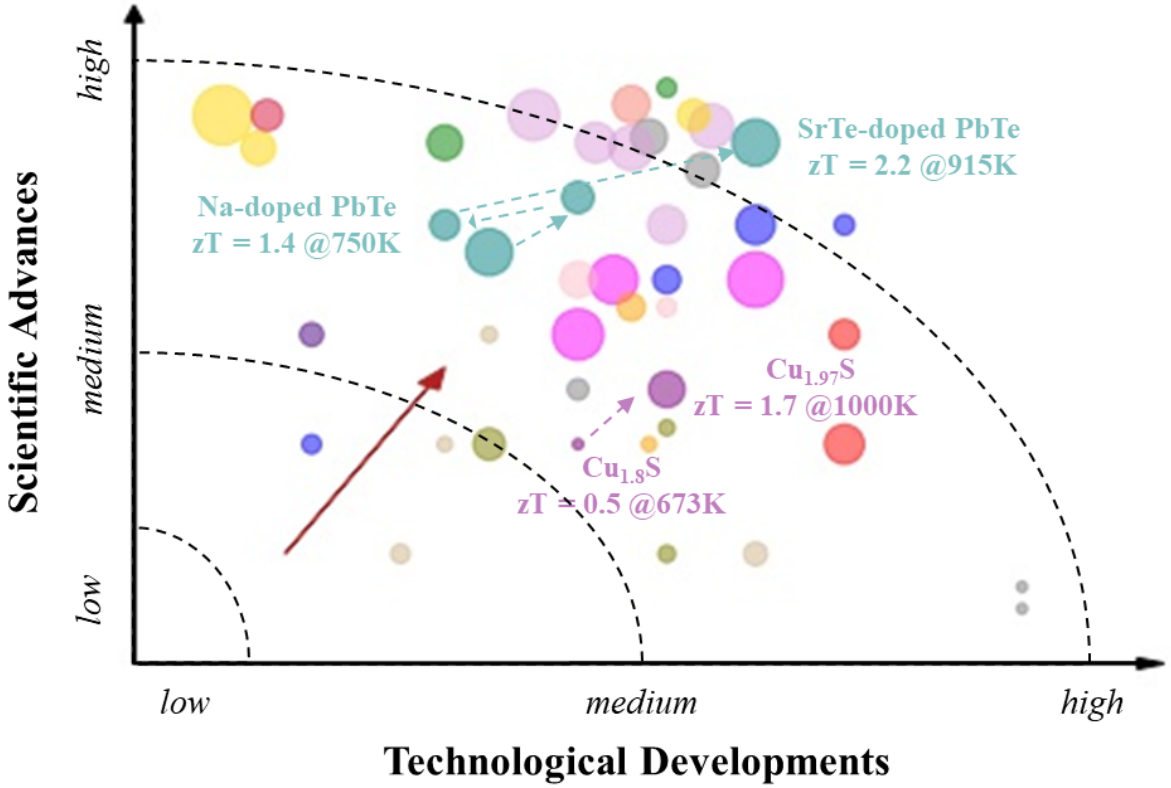

Figure 1. Path towards the accelerated discovery of new TE materials. The Y-axis ("*Scientific Advances*") represents the novelty of the physical and/or chemical strategy deployed for the attainment of high zT in a material. The X-axis ("*Technological Developments*") represents the maturity of the experimental technique used for the synthesis of a material. The size of the bubble is directly proportional to the zT_{max} in a material. However, for visualization purposes the zT_{max} have been magnified by a factor of 50. The colours have been arbitrarily chosen and they represent a class of materials (e.g. SnSe and alloys appear in yellow). The solid red arrow is a guide for the reader and points at the sector where most materials with high zT values lie. The discontinuous purple and teal arrows depict the historical evolution of a particularly chosen material. The size of the arrow's head indicates a material with higher zT.

Thermoelectric Material and Transport Descriptors

Thermoelectric (TE) descriptors allow the rapid assessment of the potential of a material by utilizing the appropriate combination of one or more fundamental parameters.[44] It is desirable to have a one-to-one correlation between the descriptor and zT.[12] Some of the TE descriptors that have been used so far are:

-***Band gap (E_g):*** The band gap of a semiconductor is defined as the difference in energy between the bottom of the conduction band (CBM) and the top of the valence band (VBM) and is important as it determines the upper limit to optimum temperature for a TE material. Goldsmith and Sharp determined that the maximum Seebeck coefficient that a material could reach at a given temperature is:

$$S_{max} = \frac{E_g}{2eT_{max}}$$

Where S_{max} is the maximum value of Seebeck coefficient, T_{max} is the absolute temperature at which S_{max} occurs and e is the electron charge. Based on this, loosely it was identified that the optimum bandgap for a TE material should satisfy the criteria $E_g > 10k_BT$.[45] However, Gibbs *et. al.* showed that significant deviations from this may occur when dealing with narrow E_g materials as bipolar conduction is not negligible.[46] Therefore, care must be taken when using band gap in identifying a promising material for a target operating temperature T.

-***Weighted mobility (U):*** Introduced by Slack and defined as:

$$U = \mu_0 \left(\frac{m_S^*}{m_e}\right)^{3/2}$$

where μ_0 is the intrinsic mobility, m_S^* is the density of states effective mass and m_e is the electron mass.[47] U is tied to a fundamental property of a material, the bond-weighted difference in electronegativity ($\Delta\chi$) between its elemental constituents.[47] Slack attributed the variation of U with $\Delta\chi$ to the difference in the bonding of the compounds. For larger values of $\Delta\chi$, the electron charge transfer between the ions is larger. For a given T, the phonons in the lattice will produce modulations in the local electrostatic field thus increasing charge carrier scattering. As a consequence, U will decrease with increasing $\Delta\chi$. Thus, in principle, the lower the $\Delta\chi$ the more promising a material is for TE applications. An intuitive correlation between weighted mobility and electronegativity difference from a chemical bonding perspective can be estimated, although the use of this is limited. Large electronegativity difference will generally result in ionic-like bonding where carriers tend to be localized and vice versa for small electronegativity difference. This is expected to affect the deformation potential which can be linked to intrinsic carrier mobility in the deformation potential scattering regime, via the following expression: $\mu_0 = \frac{\pi e\hbar^4 C_l}{\sqrt{2}m_I^* m_b^{*3/2}(k_BT)^{3/2}\Xi^2}$, where Ξ denotes the deformation potential. Since low electronegativity difference tend to result in carrier delocalization, it should qualitatively result in low deformation potential, and therefore high intrinsic mobility.

These calculations and conclusions have been derived using approaches that may not be true for all cases, such as when acoustic phonon scattering is not the dominant scattering mechanism. In a recent review, Zeier *et. al.* expanded on this approach by linking $\Delta\chi$ to the difference in energy between the atomic orbitals within the tight binding approach in binary semiconductors.[48] They also introduce the bandwidth as an important factor for predicting electronic properties in semiconductors. They go on to tie this to measurable parameters such as bond length and discuss the impact on fundamental parameters such as effective mass (m_c) and its impact on a functional property such as Hall mobility. The extension of their argumentation to ternary and quaternary systems would prove a powerful method for a descriptor for the screening of novel TE materials.

-***Thermoelectric quality factor, B or β:*** Introduced by Chasmar and Strattton [49] and later rewritten by Goldsmith and Nolas [50], it is defined as:

$$\beta = \frac{5.745\ 10^{-6}\ {m_S}^{*3/2}\ \mu_c}{\kappa_l\ T^{5/2}}$$

where μ_c is the classical mobility, κ_l is the lattice thermal conductivity and T is the absolute temperature in K. Recently, in 2013, this parameter was popularized again thanks to the work by Wang *et. al.*[44] The authors assumed that the scattering is dominated by acoustic phonons (r = -0.5) and that the bands were parabolic with a spherical Fermi surface. These assumptions allowed them to describe the quality factor, B, as:

$$B = \frac{2k_B^2\hbar}{3\pi}\ \frac{C_l/N_V}{m_C^*\ \Xi^2\kappa_l}T$$

,where C_l is average longitudinal elastic modulus and Ξ is the deformation potential. This expression is valid for materials where acoustic phonon scattering is expected to dominate throughout the whole range of T under study. However, for materials where the scattering due to polar optical phonons or ionized impurities is not negligible, this equation won't be valid and therefore cannot be used for the assessment of a potential TE candidate.

-***Fermi surface complexity factor, $N_v^*K^*$:*** Introduced by Gibbs *et. al.* this descriptor comprises the valley degeneracy (N_V^*) and the effective anisotropy (K^*)[14]:

$$N_V^*\ K^* = \left(\frac{m_S^*}{m_C^*}\right)^{3/2}$$

where m_S^* is the density of states effective mass and m^*_C is the inertial effective mass. The larger the Fermi surface complexity factor for a material, the more chances it may be a good thermoelectric material. This is because it indicates a large value of N_v^* (thus a larger number of carrier pockets are contributing for a fixed T and chemical potential) and a large value of K^* (larger deviation from the canonical spherical shaped Fermi pocket).[51] While N_v^* can be estimated directly from the bandstructure, determining K^* would require precise DFT calculation of the band structure as well as non-trivial averaging model to quantitatively represent the anisotropy factor, especially for non-parabolic band.[52]

- ***Anharmonicity:*** most of the recent achievements in TE have been due to the suppression of the lattice thermal conductivity, sometimes to the point of reaching the amorphous limit and thus approaching a phonon glass. A rather convenient way to quantify the anharmonicity in a material is by looking into the dimensionless Grüneisen parameter ($\gamma = \alpha GV/C_v$, with α the thermal expansion coefficient, G the bulk modulus, V the volume and C_v the heat capacity) , which quantifies the change in the phonon dispersion as a consequence of a change in volume.[53] In general, the larger the Grüneisen parameter the more anharmonicity is present in the material and thus the lower the values of lattice thermal conductivity, due to softer phonon modes as well as enhanced phonon-phonon Umklapp scattering.[54] Recently, Nielsen *et. al.* discussed that the lattice thermal conductivity could be also be effectively minimized in materials with lone pairs. [55] While the exact mechanism by which the lone pairs induce anharmonicity in the structure is not exempt of debate and can be material-specific, the preservation of long-range symmetry to conserve electron mean free paths, but simultaneously distorting local ordering to induce anharmonicity could provide a great knob to tune TE properties.[54]

-***Energy dependent scattering, r:*** for a real crystal (with acoustic and optical phonons, defects, impurities and grain orientations and varied grain sizes) carriers travel for certain distance (mean free path) before they are scattered. It is often useful to consider the relaxation time between collisions (τ) in its energy-dependent form:

$$\tau = \tau_0(E)^r$$

where τ_0 is the constant (energy independent) relaxation time, k_B is the Boltzmann constant, T is the absolute temperature, E is the energy and r is a characteristic exponent that describes the particular scattering. For a material in which transport happens in 3D and the bands can be modelled with parabolas, r = -0.5 for acoustic phonon scattering, 0.5 for polar optical phonon scattering and 1.5 for ionized impurity scattering.[13] Mobility and relaxation time are directly

proportional ($\mu = e\tau/m^*_C$).[13] Thus, a larger scattering time will maximize the mobility and in turn the electrical conductivity. Interestingly, in the Seebeck coefficient, the value of τ_0 does not matter and only the energy-dependence of the scattering time affects the entropy per charge. Therefore, identifying and tabulating this energy-dependence for real crystals can provide a valuable descriptor to segregate potential TE materials.

-***Electron fitness function (t):*** introduced by Xing *et. al.* this descriptor can be directly evaluated from first principles and Boltzmann transport theory, thus not requiring any experiment.[56] It is defined as:

$$t = \left(\frac{\sigma}{\tau}\right) S^2 \, N^{-2/3}$$

where N is the volumetric electronic density of states. For its calculation, the authors assume single parabolic band approximation and the constant relaxation time approximation (CRTA).

- ***Inertial Effective Mass (m_c^*)***

Building on earlier works by Gibbs *et.al.*[14], by analyzing and calculating polycrystalline averaged data mined from 1617 n-type and p-type compounds from Materialsproject.org, Suwardi *et.al.*, found that in addition to conventional understanding that low inertial effective mass results in high carrier mobility, it also facilitates sensitive power factor enhancements (i.e. given the same magnitude of band alignment, the enhancements to the power factor is larger for lower effective mass compounds).[13] This conclusion can be explained by the fact that it takes lower amount of doping to move the chemical potential of a compound with low effective mass than its heavier effective mass counterpart. Therefore, given all other parameters remain equal, the optimal carrier concentration of compounds with low effective mass is lower compared to the ones with heavy effective mass, which results in higher intrinsic mobility and thus higher power factor. It's efficacy as a descriptor was also proposed by Samsonidze and Kozinsky for half-Heusler compounds.[57]

-***Mechanical Properties:***

Significant progress has been recently achieved by obtaining high zT values for thermoelectric materials. Most of these materials, however, deteriorate at temperatures near peak zT values, which is a serious challenge to make reliable TE devices. In reality, TE materials could be

exposed to thermal and mechanical stresses which may cause reduction in device efficiency.[58] For instance, in waste heat recovery applications, sublimation of TE materials at the hot side of the device may occur, and hence, reducing the cross-sectional area at the semiconductor-metal junction, that leads to lower electrical power.[59] Therefore, considering the mechanical robustness as a design principle by the thermoelectric community will aid in obtaining robust and highly efficient TE devices. Several studies focused previously on how to experimentally measure the mechanical properties of materials.[60–62]

Mechanical properties of TE materials, such as Young's modulus, strength, fracture toughness, etc, are linked with the material's crystal structure and bonds between atoms.[60,63] For instance, the relationship between stress and strain in the linear elasticity regime is defined as Young's modulus.[58] Therefore, it would be very interesting to use the relationship between the 'macroscopic' mechanical properties and the 'atomic' level parameters, such as the change in stiffness in the material as a function of atomic displacement and establish them as screening descriptors while searching for promising candidates to ensure stable TE devices.

Now, armed with this deep understanding of TE descriptors, we progress to consider test cases of specific chalcogen-based materials and the technologies that enabled significant progress in their thermoelectric performance.

Case Studies

Case Study 1: Bismuth antimony telluride (BST)

Bi_2Te_3 was recognized as a potential layered TE material (see Figure 2(a)) in the 1950s for TE refrigeration.[64] Several material-engineering approaches have been investigated to optimize the TE performance of Bi_2Te_3 such as doping, alloying, and nanostructuring.[65] Making alloys of Bi_2Te_3 was one of the first strategies to tune its electronic properties. For instance, pressing and sintering of Sb_2Te_3–Sb_2Se_3 and Bi_2Se_3 create *p* and *n*-type Bi_2Te_3 alloys, respectively. The maximum values of the figure of merit for the *p* and *n*-type samples are 0.51 and 0.92 at 300 and 575 K, respectively.[66] After seven decades of intensive research on Bi_2Te_3, a high record zT of 1.86 at 320 K was reported for *p*-type $Bi_{0.5}Sb_{1.5}Te$ (BST, see Figure

2(b)).[67] This remarkable *zT* value was achieved by introducing dense dislocation arrays at the grain boundaries to effectively scatter phonons with a wider range of frequencies without hindering the electronic transport. Nanostructuring approach showed that the zT of BST can be improved by reducing the thermal conductivity. Poudel *et. al.* revealed that the maximum zT of 1.2 at 373 K can be achieved in nanocrystalline BST made by hot pressing nanopowders prepared by ball milling (see Figure 2(b)).[31] Furthermore, doping Bi_2Te_3 by resonant impurities such as Sn induces a sharp excess in the DOS below the valence band (~15 meV), and hence resulting in enhanced Seebeck coefficient.[68] The TE power factor can be optimized by alloying Bi_2Te_3 with Sb_2Te_3, which causes the substitution of Bi with Sb, resulting two valence maxima (with the same energy) in the electronic DOS, and therefore increasing the band degeneracy from N=6 to 12. [69] Additionally, the figure of merit of $(Bi_{0.25}Sb_{0.75})_2Te_3$ was improved by optimizing the converging valence bands of Bi_2Te_3 and Sb_2Te_3. The excess of Te was selected to tune the carrier concentration and obtaining the optimum zT of 1.05 at 300 K without nanostructuring.[70] Son et al investigated the effect of grain size in *p*-type bismuth telluride alloy made by sintering. They optimized the grain size by controlling the ball milling time, which in principle revealed how grain size rules thermal transport, and hence *zT* of 1.14 was found near room temperature.[71]

Hence, in the case of Bi_2Te_3/Sb_2Te_3 and their complementary alloys, zT has gone up from 0.5 to 1.8 over a span of seven decades (see Figure 2(c)). The key advancements have been both a combination of novel physics such as DOS distortion, band convergence, phonon scattering by nanostructuring as well as new processing techniques such as spark plasma sintering, and nanostructuring through milling. This is an example where even in well-established material systems, there is room to explore new phenomena in physics, where process innovation has been a key driver to push the *zT* up by 400%. This case study provides a prime example of a known material system springing surprises over many decades, and we can predict that using machine learning, high-throughput experiments and process optimization, similar development of other known material systems could potentially be sped up significantly with the use of new tools.

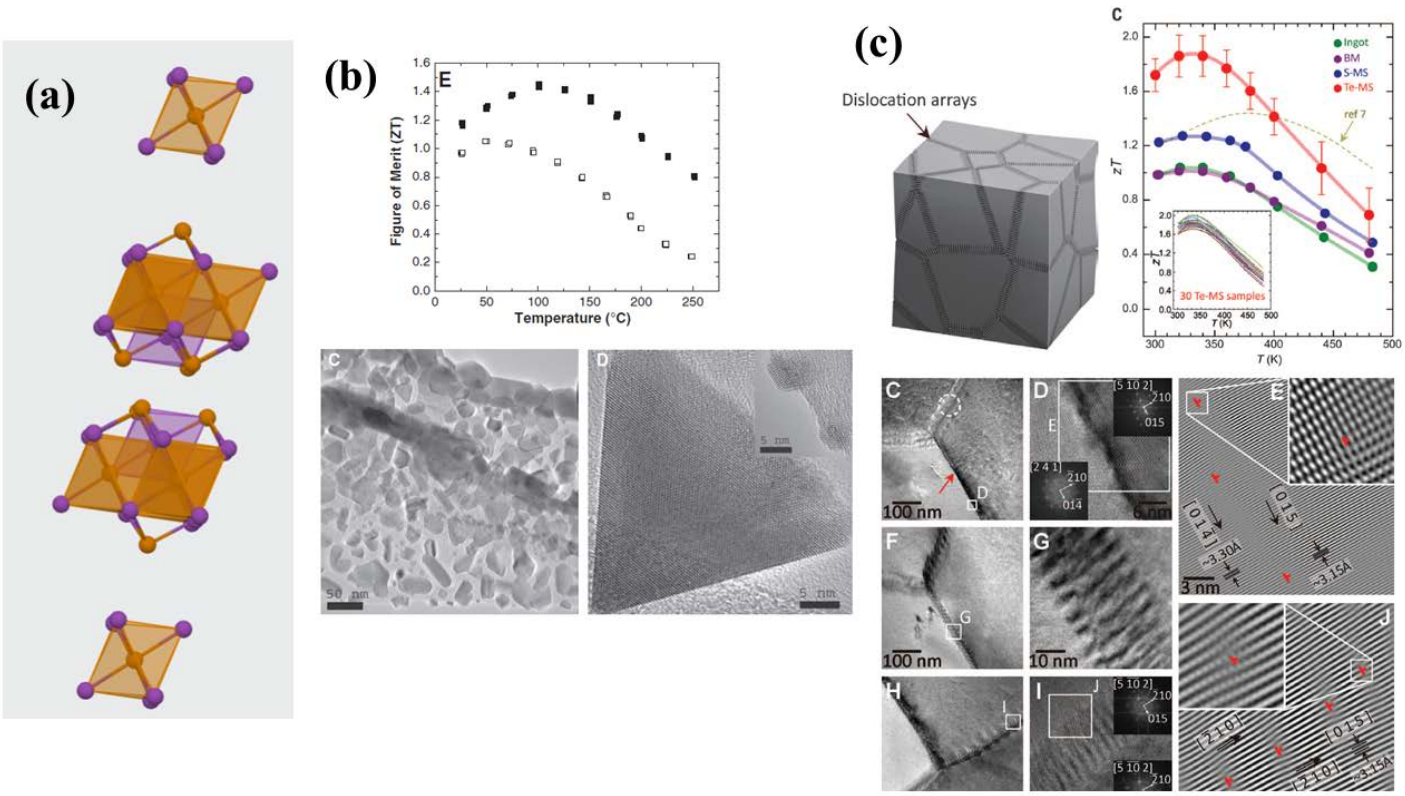

Figure 2. (a) Layered crystal structure of Bi_2Te_3 (space group $R\bar{3}m$ [166], with Bi and one Te atom in Wyckoff position 3a and the other Te atom in 6c) (b) Nanobulk Bismuth antimony telluride (BST), from Poudel *et.al.*[31]with a zT of 1.2 at 373 K, reproduced with permission from The American Association for the Advancement of Science and (c) Dense dislocation arrays in BST, zT of 1.86 at 320 K, from Kim *et. al.* [67] Reproduced with permission from The American Association for the Advancement of Science.

Case Study 2: Lead/tin telluride/selenide (Pb/Sn-Te/Se)

Lead telluride was first implemented in TE generators by A. F. Ioffe in 1928.[72] After that, the radioisotope TE generator (RTG) based on PbTe was announced.[73] Two decades later, many TE studies on PbTe appeared.[74,75] However, accurate measurement of z*T* for PbTe at the temperature of interest (around room temperature and above) was limited as no precise thermal conductivity setup was available. In the early 1960s, the flash diffusivity method was developed, and by that time, the interest of the thermoelectric community on PbTe shifted away.[76] After the seminal work by Hicks and Dresselhaus in 1993,[77,78] which indicated nanostructuring could enhance the TE performance by taking advantage of discretized electronic DOS, many reports were published confirming verifying this theoretical prediction. Building upon this, a prominent enhancement of the TE performance in PbTe was

demonstrated by the distortion of the electronic DOS by incorporating thallium impurity levels, where purportedly the Thallium impurity level introduced resonant scattering, thus enhancing the Seebeck coefficient significantly, as shown in Figure 3(d).[79] Subsequently, a z*T* of 2.2 at 800 K was obtained for $AgPb_mSbTe_{2+m}$ due to concurrent enhancement in electrical conductivity and Seebeck coefficient, which was attributed to the change in the DOS structure and the effective doping.[80]

In 2012, Biswas *et al* demonstrated mesoscale engineering of nanostructured PbTe to improve the zT further (2.2 at 915 K, see Figure 3(b) and 3(c)). This high z*T* was obtained due to the huge reduction in the lattice thermal conductivity by scattering phonons with a broad frequency spectrum in a hierarchical nanostructuring approach.[81] Very recently, Liu-Cheng Chen et al have shown that a prominent enhancement in zT (1.7 at room temperature) for Cr doped PbSe can be achieved by applying external pressure. They attributed this enhancement to the topological phase transition driven by the external pressure that promotes electrical conduction.[82]

Structurally analogous to PbTe (see Figure 3(a)), tin telluride (SnTe) has attracted a lot of attention due to its potential to perform as well as PbTe, with the benefit of being lead-free and therefore non-toxic.[83] The lower performance of SnTe has been attributed to a larger valence band offset between the light-hole L band and the heavy hole Σ band, when compared to that of PbTe (0.30 eV and 0.15 eV, respectively), hindering band convergence and thus reducing the maximum power factor *via* reduction of the number of available valleys (N_v). In addition to this, SnTe has an intrinsically high concentration of Sn vacancies, leading to overdoping and high thermal conductivity.[84] However, researchers have deployed a plethora of strategies in order to enhance the performance of SnTe. One of the very first strategies was the introduction of nanostructures, that would act as phonon scattering centres and reduce the lattice thermal conductivity. Tan *et. al.* showed that alloying with 3% mol Cd, band convergence can be achieved and moreover, introducing endotaxially nanostructured CdS effectively suppresses phonon scattering and therefore reduces the lattice thermal conductivity. The combination of these strategies led the authors to a zT of 1.3 at 873K.[84] In addition, synergistic band engineering in addition to a clever manipulation of the intrinsic defects has been proved effective to this end. Tang and co-workers demonstrated that alloying SnTe with 5% of GeTe increases the solubility of the SnTe-MnTe alloy, with an overall reduction of the band offset, thus achieving band convergence and increasing the power factor. In addition, alloying with

Cu_2Te reduces the lattice thermal conductivity down to its amorphous limit, rendering a zT of 1.8 at 900K.[85]

Hence, in the cases of PbTe/Se and SnTe, higher zT has mostly been enabled by the emergence of new physics coupled with materials engineering to control charge and phonon scattering. This presents a case where seeding and testing of new ideas is necessary to push the boundaries of knowledge in existing materials, similar to the BST case study.

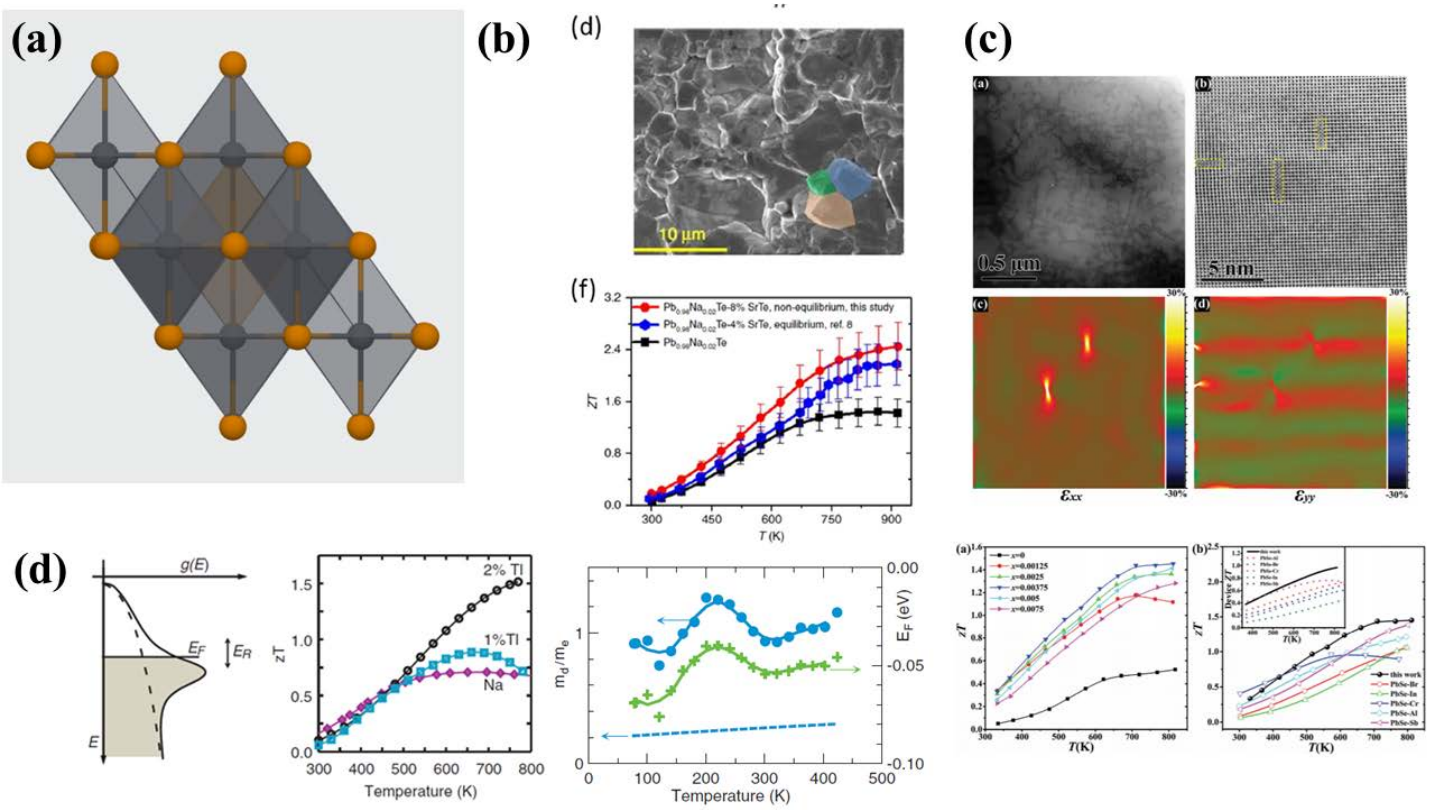

Figure 3. (a) Crystal structure of PbTe, (b) Hierarchical nanostructured PbTe, from Xiao *et. al.*[86],reproduced under a Creative Commons Attribution 4.0 International License (https://creativecommons.org/licenses/by/4.0/) (c) Hierarchical phonon scattering and dynamic doping in PbSe, from You *et. al.*[87], reproduced with permission of the Royal Society of Chemistry. (d) distortion in the density of states of PbTe induced by Tl doping, from Heremans *et, al.*[79] Reproduced with permission from The American Association for the Advancement of Science.

Case Study 3: Germanium Telluride (GeTe) and Tellurium Antimony Germanium Silver (TAGS)

GeTe-based compounds (TAGS – Tellurium-Antimony-Germanium-Silver) have been identified as potentially good thermoelectric[88] since 1960s[89] and has been widely explored

recently.[90] In terms of application, it was used as RTG in Pioneer10 space probe to Jupiter and numerous space-applications afterwards. It was mainly explored as an isostructural (see Figure 4(a)) alternative to the toxic PbTe (at high temperature) and the lack of high temperature stability of p-type PbTe. Alloy of (0.15) $AgSbTe_2$ – (0.85) GeTe (TAGS 85) was found to display robust high temperature performance as well as relatively low thermal expansion coefficient (15 x 10-6 K-1 compared to 29 x 10-6 K-1 for PbTe) which is beneficial for mechanical stability at high temperature.[89] Unlike SiGe, TAGS was mainly used for intermediate temperature application (below 525 C) due to its low phase transition temperature (510 K) and high sublimation rate at high temperature, compromising its compositional stability.

The rationale of alloying GeTe with AgSbTe2 were due to the fact that pristine GeTe has low power factor due to excessive carrier concentration induced by Ge vacancies.[91–94] In most studies and applications, the process condition used was mainly melting stoichiometric amount of alloy ingot in ampules since sintering and cold pressing were found to be unsatisfactory for fabricating TAGS legs.[89]

Prior to 2008, most works on TAGS were based on the concept of alloying-induced lattice strain which leads to low lattice thermal conductivity. Hence, most reports were focused on the phase transformation (see Figure 4(b)) and thermoelectric properties of these system, not on the process related microstructure.[95,96] In 2008, Yang et. al examined the effects of the microstructures of TAGS by quenching and pulverizing molten ingots into micron sized particles followed by hot pressing. It was found that in situ formed nanodomains and inhomogeneities in the order of 10 nm was the main reason for low thermal conductivity in this system.[97] Subsequently, carrier and phonon engineering with $AgSbTe_2$ alloy lead to high performance by simultaneously optimizing carrier concentration and introduces phonon scattering centres through alloying.[98–101] Similar enhancements were achieved by alloying GeTe with AgBiTe2, Bi2Te3, In2Te3, $Bi_2Se_{0.2}$,$Te_{2.8}$, and Sb_2Te_3 (see Figure 4(c)).[102–110] In order to scatter high frequency phonons, doping of heavy elements such as Bi, Pb, Sb and Mn to generate mass fluctuation that can act as point defects that reduces the lattice thermal conductivity.[102–105,111,112] For instance, $Ge_xPb_{1-x}Te$ solid solution increases zT due to donor dopant nature of Pb (which shifts the excessive acceptor concentration in pure GeTe to a more optimal level) and reduced thermal conductivity due to nanoscale modulations.[104] Very recently, heat treatment was shown to be a viable strategy in suppressing Ge phase aggregation and uniformly distributing Ge precipitates that yield synergistic results in all-scale phonon scattering as well as optimized doping.[113]

In addition to de-doping of GeTe, parallel efforts to improve the Seebeck coefficients such as introducing resonant states by introducing Dy in $AgSbTe_2$-GeTe[114] as well as Ce and Yb in TAGS-85 was reported.[115] Furthermore, band convergence was achieved by doping 3 mol% Bi_2Te_3 into $Ge_{0.87}Pb_{0.13}Te$.[116]

Hitherto, the record breaking zT of 2.4 at 600 K for GeTe based compound was reported by Yanzhong Pei, *et.al.* in 2018. By utilizing slight symmetry-breaking near the rhombohedral-cubic transition temperature to synergistically achieve band-convergence and reduce lattice thermal conductivity.[117,118] This is an incredible study considering the processing condition was simply using hand ground and hot pressing. More recently, crystal-field engineering and ferroelectric instability has been touted as another route to improve the performance of GeTe.[119] Last but not least, entropy engineering (by increasing configurational entropy via alloying) have also be shown to improve power factor.[120,121]

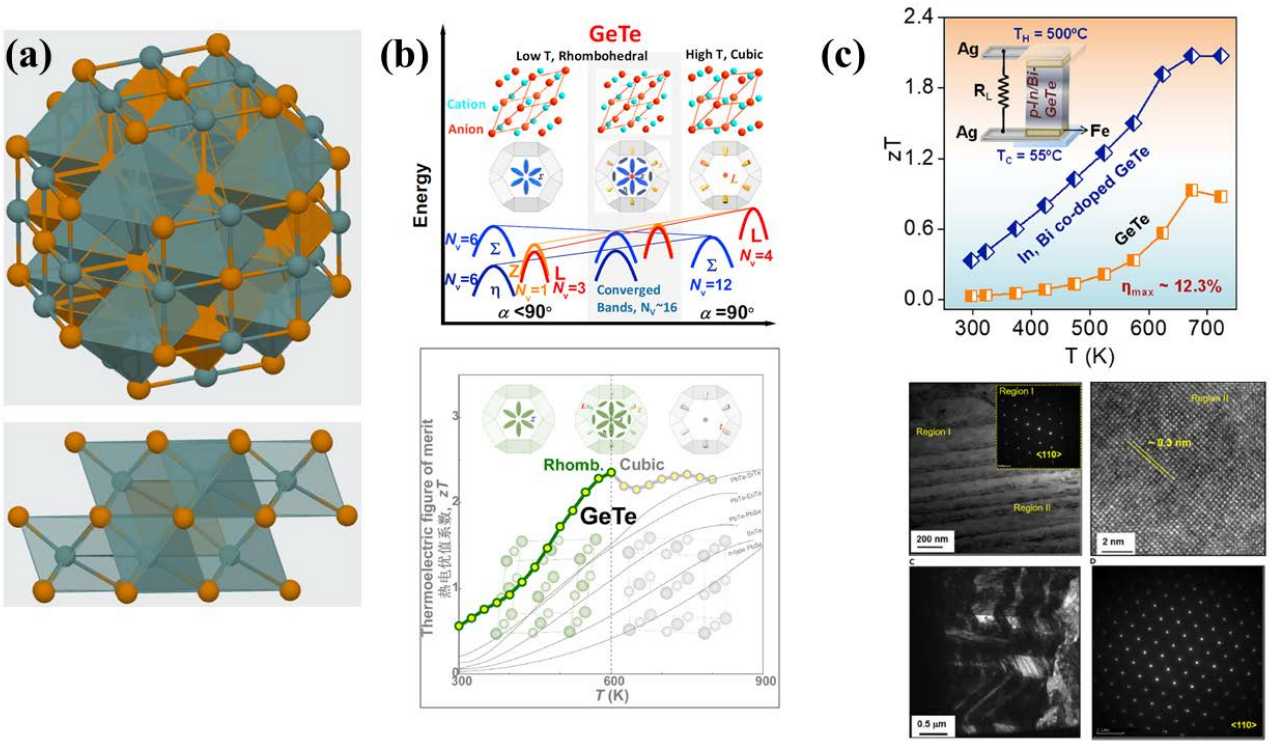

Figure 4. (a) Crystal structure of GeTe, showing Fm-3m high temperature cubic phase (top) and R3m low temperature rhombohedral phase (b) Band convergence in GeTe, from Li *et.al.*[116] Reproduced with permission from Elsevier. (c) Bi and In co-doping in GeTe, from Perumal *et. al.*[122] Reproduced with permission from Elsevier.

Overall, over the years, breakthroughs in scientific understanding (e.g. alloying and doping to optimize carrier concentration, band convergence, and phonon-scattering) has enabled the zT of this material system to increase dramatically. More importantly, some of the new scientific

breakthroughs (i.e. nanoscale grains to scatter phonons) were enabled by adoption of relatively mature technologies (i.e. ball milling, spark plasma sintering) that subsequently enabled scientists to investigate new physical mechanisms to improve the thermoelectric performance.

Case Study 4: Silicon-Germanium (SiGe)

An example of a traditional compound which has wide range of applications can be found in cubic SiGe (See Figure 5(a)).[123] SiGe is a tried and tested compound with primary application in radioisotope thermoelectric generator used by NASA in 1976.[59,124] The main draw to using this compound lies in its high temperature mechanical and performance stability (up to 1300 K). In the early days, hot pressing was mainly used to fabricate polycrystalline bulk while preparation from melts was used for the study of silicon-germanium mixed-crystals or "alloys" as possible materials for thermoelectric generators by Ioffe and Ioffe. Initially, powder metallurgy (hot pressing) was intended as a way to change carrier concentration, as the dopant solubility changes near the liquidus line. Later, this powder metallurgy processing was used to improve electrical properties via density increase as well as decreased thermal conductivity via optimizing grain size. With the evolution and advancements of materials processing technologies, higher performance SiGe were obtained using the combination of mechanical alloying + powder metallurgy (SPS).[125,126] The evolution of processing technique for this compound can be summarized as follows:

Preparation or alloying from melts (single crystal) → Powder metallurgy process → Mechanical Alloying (i.e. ball milling) → Thin films/superlattices.

In terms of thermal transport, the lattice thermal conductivity of SiGe mixed crystal was found to be lower than its respective parent pure crystals, reaching the alloy limit[39], while the carrier mobility was found out to be just slightly lower, which justifies the alloying of Si and Ge.[127] The resulting optimal zT at that time were 0.5 (p-type) and 0.9 (n-type).[89] In 1978, Pisharody and Garvey proposed that dissolving small amount of GeP into SiGe to further reduce lattice thermal conductivity.[128] However, no reduction in thermal conductivity was observed: instead, adding GeP inadvertently optimized the carrier concentration and hence zT.

As technologies progressed, nanostructuring in the form of SiGe superlattices to exploit quantum effects was studied. Advancements in vacuum systems enabled Superlattices of SiGe to be grown from as early as 1970's via ultra-high vacuum evaporation techniques.[129] Later on, with the advent of Molecular Beam Epitaxy, more precise control of composition and thickness could be achieved. Building upon the physical intuitions derived from nanostructuring techniques, then-record zT for nanostructured bulk p-type and n-type SiGe bulk alloys of 0.95 and 1.3, was achieved in 2008 and 2009, respectively.[130–132] The spectacular progress in zT enhancement owes a lot to a key development in materials processing: advancement in ball-milling, which enables nano-grains to be achieved. This, combined with other state-of-the-art process back then (DC hot-press) was used to form nanocrystalline alloys. In retrospect, both hot pressing and mechanical alloying have already existed for more than 20 years by this point in time. To date, the record zT for bulk material ~ 1.84 for *n-type* SiGe at 1073 K was achieved by multi-frequency (broadband) phonon scattering using the combination of point defects, dislocations, and grain boundaries (see Figure 5(b) and 5(c)).[124] In the case of SiGe, like other material case studies, technological progress indeed enabled new scientific directions that were previously not accessible.

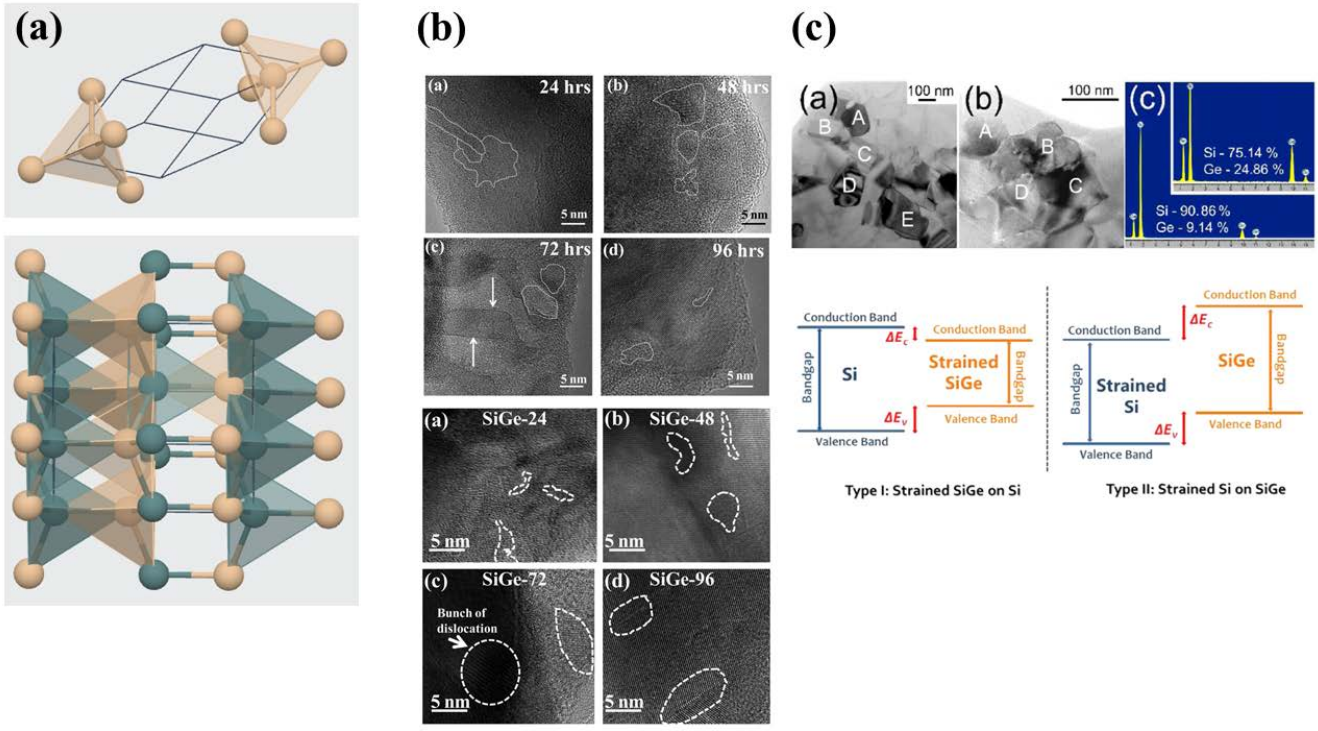

Figure 5. Crystal structure of (a) Si showing cubic Fd-3m structure and (b) SiGe showing hexagonal P63mc structure, (b) TEM images of SiGe alloy samples prepared using different conditions, from Basu *et. al.*[124] Reproduced from permission of the Royal Society of Chemistry. (c) TEM images, EDX spectra and band diagram from doping modulated SiGe, from Yu

et.al.[132] Reproduced from Yu, B.; Zebarjadi, M.; Wang, H.; Lukas, K.; Wang, H.; Wang, D.; Opeil, C.; Dresselhaus, M.; Chen, G.; Ren, Z. Enhancement of Thermoelectric Properties by Modulation-Doping in Silicon Germanium Alloy Nanocomposites. *Nano Lett.* **2012**, *12* (4), 2077–2082. Copyright 2012 American Chemical Society

Emerging materials

Tin Selenide (SnSe) and Tin Sulphide (SnS)

Tin selenide (SnSe) is a layered orthorhombic material that historically, unlike other traditional TE materials like PbTe or Bi_2Te_3, has been less explored.[133,134] It was prepared for the first time by Albers *et. al.* in 1962, employing traditional single crystal methods, and not much work was done thereafter. [135,136]

In 2014, Zhao *et. al.* reported an ultralow lattice thermal conductivity in pristine single crystals along the b-axis (≈ 0.23 W m^{-1} K^{-1} at 973K). They selected this material because traditionally, materials with layered structures (such as Bi_2Te_3) are good TE materials. In the case of pristine SnSe, a zT of 2.6 ± 0.3 at 923 K was achieved as a consequence of the large anharmonicity and anisotropy in the strong covalent bonding between Sn and Se in the b-axis.[137] The same authors, two years later and employing the same technique, managed to introduce sodium (Na) as hole dopant, increasing the value of zT average but without further increase in zT_{max}.[138] Other than Na, only silver (Ag) was found to be a good dopant for SnSe. Chen *et. al.* deployed a melting and hot-pressing strategy for the doping of polycrystalline bulk SnSe with 1% mol Ag, reporting a zT of 0.6 at 750 K.[139] Regarding n-type SnSe, Duong *et. al.* introduced Bi on the Sn site and reported a zT of 2.2 along the b-axis at 773 K for n-type SnSe single crystals.[140] Advances in processing operations and synthesis techniques, such as ball milling (BM) and spark plasma sintering (SPS), made possible the move away from single crystal materials, synthetized with traditional techniques (melting or Bridgman synthesis). Remarkable progress in polycrystalline SnSe were demonstrated by combinations of alloying and hot pressing. Lee *et. al.* achieved the zT ≈ 2.50 - 2.7 at 800K, record for polycrystalline SnSe, by alloying with 5% PbSe and introducing 1% mol of Na as p-type doping. The key in their success was the chemical reduction of SnO and SnO_2 by annealing in a reductive atmosphere.[141]

Very recently, Chang *et. al.* deployed a band convergence strategy in single crystal SnSe to break the record zT. The synergistic enhancement of m* without a dramatic decrease in mobility, combined with a suppression of the thermal conductivity due to softening of optical phonons enabled them to reach the current zT record of ~2.8 ± 0.5 at 773 K for n-type single crystal SnSe (see Figure 6 (a)).[41] Similar work was conducted by He *et. al.* for the synthesis of low cost, Earth abundant $SnS_{0.91}Se_{0.09}$ single crystals and found that Se had the same effect that Br in SnSe: it enabled the two-band convergence, two-band divergence, and two-band crossing interplay (see Figure 6(b)) that led to a zT_{max} of 1.6 at 873 K.[142]

Thus, we conclude that the combination of new chemical phenomena (large bond anharmonicity in the b-axis) and the synthesis of high-quality samples by means of a mature technology are the main driving forces for the discovery of the material with highest zT at the moment. This is in line with our observations from Figure 1 and reinforces the idea that new, high performing TE materials are to be explored by scientific advances as opposed to technological.

Magnesium antimonide and alloys (Mg_3Sb_2 – Mg_3Bi_2)

Magnesium antimonide (Mg_3Sb_2) and its alloys are a recent material that is set to substitute bismuth telluride and its alloys for low T applications.[143] The main factor hindering the replacement is the complex synthesis and processing of the compounds, as the high vapour pressure and causticity of Mg introduces defects and boundary phases that have a negative impact on the transport properties.[144,145] Most of the efforts have been centred on classical alloying approaches in order to reduce the thermal conductivity and increase the grain size, thus improving the electrical properties. Shi *et. al.* utilized a combination of melting, annealing and hot pressing to achieve a zT of 1.1 in the 300K-500K range for the n-type Sc-doped Mg_3Sb_2−Mg_3Bi_2 alloy. This was realized due to the coarse-grain structure enabled by the synthesis and processing conditions.[146] Another step towards better performance in Mg_3Sb_2 was achieved by simply changing the processing conditions, revealing that a clever optimization of the synthesis is a key parameter for obtaining high performance TE materials.[147] Here, Shi and co-workers employed tantalum tubes as sealing units for melting of the elemental precursors for the synthesis of polycrystalline $Mg3.05Sb_{2-x-y}Bi_{y-x}Te_x$ ($x \leq 0.04$,

$y \leq 1.5$) alloys. This sealing prevents oxidation during hot press sintering and Mg from evaporating, thus reducing the vacancies that could be created. This led to an enhancement in mobility due to the reduction of grain boundaries, that enabled them to achieve a zT of 0.72 at 300K and a zT_{max} of 1.31 at 500K.[148] Since the seminal work of Pei *et. al.*[10], describing how band engineering could boost the performance in bulk TE materials, multiple efforts have been carried out in order to achieve band convergence in Mg_3X_3(X = Sb, Bi) and alloys. Imasato *et. al.* alloyed Mg_3Sb_2 with Mg_3Bi_2 in order to decrease the conduction band mass to the point where there is a band crossing between the CB (Γ) and a neighbouring band (with $N_v = 6$). This happens when 70% of Mg_3Bi_2 is introduced in the alloy, leading to a $zT \approx 0.8$ at 350K.[149] However, the Zintl phase that is the closest to replace bismuth telluride for room temperature applications is a Mg_3Bi_2 alloy, that shows zT = 0.9 at 350K. Mao *et. al.* reported this figure-of-merit for the n-type $Mg_{3.2}Bi_{1.498}Sb_{0.5}Te_{0.002.}$ This is due to the semi metallic character in which the Seebeck coefficient is large due to the disparity in the mobility between electrons and holes, caused by the anisotropy in the density-of-states effective mass, as seen in Figure 6(c) and (d).[150]

This case study is a prime example of how when a new material is discovered enabled by new physics, existing processing techniques and technological advancements can be adopted quickly to further optimize the TE properties.

Discussion

Our case studies reveal that breakthroughs in thermoelectrics mostly seem to emerge from new scientific ideas when supported by technologies that are moderately evolved; for instance a brand new technology would not (by itself) be sufficient to push an existing material towards high values of zT – therefore materials discovery via new physics, especially of non-equilibrium charge scattering and material/transport descriptors remains the key advancing step. This is consistent with our conclusion from Figure 1, where novel materials and novel physics and chemistry insights are the hardest step and require the added acceleration that can possibly be provided by machine learning, high-throughput calculations and experiments. Process parameter optimization, while an important step, typically happens on a shorter timescale; while this can also benefit from machine learning optimization and design of experiments, it is not the bottleneck.

It is also to be noted that in terms of device fabrication, manual *p* and *n* legs in series have been the tried and tested method for decades of thermoelectric device applications. More recently, some emerging techniques have been developed including electrochemical deposition-based technique to fabricate micro-legs[151], CMOS fabrication techniques[152], and 3D printed legs.[153] With the advancement and expected maturity of 3D printing technologies, we expect it to play a pivotal role for large scale, facile thermoelectric device fabrication in the near future.

To this end, it is highly encouraging that many recent reports in thermoelectric research go beyond reporting zT to include device characteristics as well as efficiency.[150] For instance, either power generation or cooling performance can be included to support the claim for zT and applicability of the thermoelectric material for a real-world application. This serves a dual purpose: as a confirmation for the reported zT as well as going further to demonstrate viability of device fabrication. In addition, in the presence of good device models, as is possible in thermoelectrics, machine learning can be used to perform system level diagnostics to directly determine limiting factors affecting device performance (such as large contact resistance, imperfect load matching conditions, etc.[154])

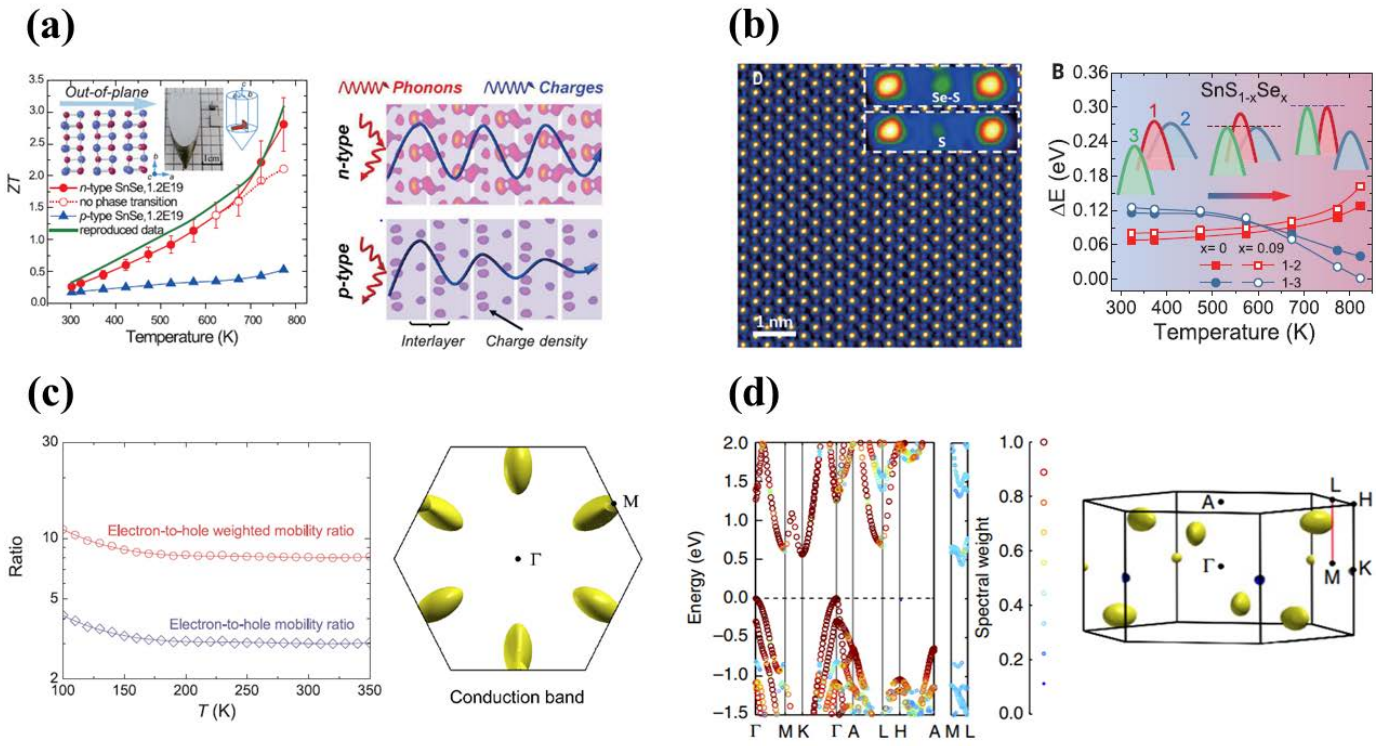

Figure 6. (a) Physical representation of the selective scattering of charge carriers and phonons and zT of SnSe, from Chang *et. al.*[41] Reproduced with permission from The American Association for the Advancement of Science. (b) difference between Se-substituted S and the SnS matrix as per STEM HAADF and pictorial representation of dynamic evolution of three separate valence bands with increasing temperature for SnS, from He *et. al.*[142] Reproduced with permission from The American Association for the Advancement of Science. (c) Disparity between charge carriers in Mg_3Bi_2 and calculated Fermi surface for the conduction band, from Mao *et. al.*[150] Reproduced with permission from The American Association for the Advancement of Science. (d) Effective band structure of $Mg_3Sb_{1.5}Bi_{0.5}$ solid solution and calculated Fermi surface for n-type Mg_3Sb_2, from Zhang *et. al.*[155] Reproduced under a Creative Commons Attribution 4.0 International License (https://creativecommons.org/licenses/by/4.0/).

Data Driven Approaches

With open source materials databases becoming more available and machine learning reaching maturity, we live in a privileged era of identifying key parameters that comprehensively describe thermoelectric materials (i.e. descriptors), leveraging upon existing physical understanding to derive new physical insights. A good example of the state-of-the-art physical insights based on data-driven study is the fermi surface complexity factor ($N_V^* K^*$).[14] The efforts to discover compounds with high $N_V^* K^*$ values was built on earlier work in high-throughput thermoelectric compounds screening using DFT and BoltzTraP.[14,156,157] Other efforts focused on band-structure as descriptor.[158] While $N_V^* K^*$and band-structure are relatively insightful electronic descriptors for thermoelectrics, their interdependence with the scattering times renders them less comprehensive. A more recent study using the same dataset reveals the important role of inertial effective mass in obtaining both high $N_V^* K^*$ and sensitive enhancements to power factor via band alignment.[51] It is important to qualify that at this stage, these data-driven insights are still largely DFT-based with some coarse assumptions (i.e. constant carrier relaxation time approximation as well as a rigid band). A more powerful approach can be envisaged by taking into account the electron-phonon interaction in the transport calculations that may give more realistic values of thermoelectric parameters, especially carrier mobility. Furthermore, recent reports using intuition-agnostic approaches based on unsupervised machine learning of word-embeddings from materials science literatures predicts several high performance thermoelectrics such as $CuBiS_2$, $CsGeI_3$, and $TlSbSe_2$ that traditionally have never been reported in any thermoelectric literatures.[33] In addition, the idea of creating a comprehensive experimental database is alluring, yet a gargantuan undertaking. Mapping out the entire stoichiometric space for inorganic compounds by utilizing key chemical concepts and elemental attributes is one approach to overcome this

complexity, allowing for advances in machine learning to pick out irreducible representations that can connect process to structure to property.[159] Overall, in addition to technological and scientific progress, creation and use of materials data provides a new dimension of discovery that can potentially lead to both new materials as well as new scientific/physics discovery.

Theoretical Calculations and Machine Learning for Predicting Efficient TE Materials

Theoretical calculations represent an essential step that inspires experimentalists to investigate research on promising candidate of thermoelectric materials. For example, the remarkable work by Dresselhaus *et. al.* drove research in the thermoelectric community towards nanostructuring to promote discretization in the electronic density of states that were expected to lead to superior TE performance.[78] Furthermore, complex TE materials (such as skutterudites, clathrates and Zintl phases) had been predicted to exhibit exceptional performance by breaking the intercorrelation between transport properties that determine zT.[2] In the previous decades in the history of TE research, conventional methods of theoretical calculations (such as density functional theory, molecular dynamics, etc) have been usually reliable options to predict or explain rigorously the interesting transport phenomena in TE materials. However, they are computationally expensive with limited scope of screening in the space of materials.

Recently, there have been several attempts to utilize machine learning tools to uncover non-traditional TE materials that surpass their traditional counterparts, that may not be captured by human intuition.[160] For instance, using materials descriptors[161] and deep neural networks to predict stability of mixed garnets and perovskites,[162] graph-based neural networks for inorganics[163] as well as organics[164] are some examples of using machine learning approaches to predict ground-state properties of materials. However, predicting functional properties such as in thermoelectrics, where charges and phonons are out of equilibrium, requires better datasets for machine learning approaches to learn from and are still in their infancy.[165,166]

Machine Learning and Process Optimization towards Inverse Design

Traditional characterization tools, which can investigate a wide range of physical properties (surface morphology, crystal structure, electrical/magnetic, optical properties etc), have played essential roles in understanding the structure-property correlation, and hence theories and

models were established. However, in the era of Artificial Intelligence (AI) and ML, beside high-throughput (HT) materials synthesis or processing, HT characterization is the need-of-the-hour to either test existing hypotheses or discover new phenomena. The current challenge is to make HT synthesis and characterization tools that can contribute effectively to accelerating research outputs. Piotr S. Gromski et al have proposed a universal approach (*Chemputer*) for chemical synthesis and discovery by having robots that can investigate chemical reactions and data analysis in a much faster manner than manual methods. By integrating multiple characterization tools in the loop, extensive size of data can be generated that would be fed into optimization algorithms to explore the multidimensional space of the chemical reactions.[167] Furthermore, Macleod and his co-workers could assemble a self-driving laboratory (*Ada*) that is dedicated for advancing the performance of organic thin films for solar applications. With the help of Bayesian optimization algorithm in the loop, Ada can explore and predict the new experimental parameters from the vast multidimensional space.[168] By combining machine learning methods and domain expertise, inverse design is anticipated to tackle research problems very efficiently via creating new materials or molecules with desired properties and functionalities. For instance, Kumar et al have predicted and synthesized 17 novel polymers with desired cloud point temperatures ranges from K with a high accuracy that is limited to the systematic error in the experimental setup.[169] One of the key points of performing inverse design problems, along with having machine learning tools, is to be able to propose accurate materials descriptors that lead to superior properties. Such an integrated high-throughput screening approach has seen very promising initial success, for instance in molecular organic Light-Emitting Diode molecules[170], and its proposed approach to energy materials .[171,172]

Thus, with the emergence of HT synthesis methods and self-driven laboratories, the classical Edisonian approach to materials discovery has been progressively abandoned, in pursue of a better, more efficient method.[173] Despite the recent boom, combinatorial methods, embodying rapid synthesis and simultaneous, on-line tools for diagnosis are not brand new, having their origin in the phase diagram studies, back in the 1960s.[174] Historically, one of the first cases of combinatorial science applied to the discovery of solid-state inorganic materials is registered in 1995, when Xiang *et. al.* developed a mask-enabled physical evaporation technique for the discrete deposition of superconducting oxide thin films.[175] Their work produced a 128-member library and led to the discovery of two superconducting oxides ($BiSrCaCuO_x$ and $YBa_2Cu_3O_x$).

Many combinatorial approaches have been focused on oxides, with special mentions to efforts to replace amorphous SiO_x as dielectric were conducted by van Dover and collaborators and the investigation on crystalline high-K dielectrics by Chang *et. al.*[176,177] However, no combinatorial method is complete without a high-speed characterization technique.[178] Thus, it is crucial to *identify a descriptor (*see "Thermoelectric Material and Transport Descriptors" section earlier*) that evaluates the potential of a material for a specific application and develop a characterization technique for its rapid, accurate measurement.* Danielson *et. al.* developed an automated combinatorial synthesis and characterization for the discovery of new luminescent materials. They deployed a combination of mask-assisted electron beam evaporation for the synthesis and high- throughput imaging of the visible spectrum with a CCD camera for optical characterization. Their work led to a discrete library consisting of 25,000 different oxides and the discovery of a new red phosphor ($Y_{0.845}Al_{0.070}La_{0.060}Eu_{0.025}VO_4$) with quantum efficiency of 0.83 ± 0.04, comparable to the then state-of-the-art material.[179] More recently, Mao developed a combinatorial approach for the synthesis and characterization of photovoltaic materials as well as transparent conducting oxides. Their work is outstanding for many reasons, one of which being the fact that they developed systems for material characterization (band gap) and characterization of the functional property of the material (carrier mobility and lifetime).[180] Most combinatorial synthesis approaches use physical methods for synthesis. In addition to evaporation, pulsed laser deposition is often used for epitaxial growth of oxides.[181] All these techniques rely on vacuum technology, which increases both cost and synthesis/characterization time. Chemical methods such as continuous hydrothermal flow synthesis can alleviate these problems thanks to their atmospheric pressure operation and their ease to scale up, thus accelerating the commercialization of the materials.[182,183] Another alternative that has been deployed recently by Kremsner *et. al.* is microwave-assisted synthesis.[184] Whilst chemical methods offer the advantages of scalability and user-friendly operation conditions, they normally render materials with lower quality (compactness, adherence to the substrate, mixed phases) than the materials obtained by their physical synthesis counterpart methods. Therefore, a compromise between synthesis time/cost, material quality and scalability need to be reached before designing any combinatorial approach.

Developments in combinatorial synthesis for thermoelectric film materials have been very recently published by Adamczyk *et. al.*[185] They utilized an aerosol spray for the high-throughput deposition (very high rates of near 1 μm min^{-1}) of PbTe-SnTe thick films (*ca.* 10

μm) on Al_2O_3 that were subsequently annealed in fused silica ampoules. They conducted conventional material (Scanning electron microscope, X-ray spectroscopy and X-ray diffraction) and thermoelectric characterization (Seebeck coefficient and electrical resistivity). They concluded that the properties have a positive correlation with bulk samples and that after an optimization of the aerosol deposition conditions, it is a potential candidate for the high-throughput discovery of new thermoelectric thin films. However, the best commercially available TE materials yet remain bulk samples. This is due to the superior quality of bulk samples (dense, homogeneous composition) as opposed to thin films (porosity, element segregation leading to compositional inhomogeneities). Ortiz *et. al.* led an effort to achieve HT synthesis of bulk TE. A combination of automation of powder dispensing and parallelization of hot pressing and ball milling led to the astounding 5-10x increase in synthetic speed, obtaining 121 bulk samples within the PbTe-PnSe-SnSe-SnTe system.[42] They performed non-HT characterization in order to determine the quality factor (β) of the samples and represented the results in the form of heat maps. They arrived at the non-intuitive conclusion that the best performing alloy ($Pb_{0.7}Sn_{0.3}Te_{0.9}Se_{0.1}$) does not lie along any intuitive set of compositions. This demonstrates that HT experimentation is a useful tool to achieve process optimization as well as discovery of new, non-intuitive materials. Therefore, we expect that the combination of machine learning optimization, coupled with high-throughput calculations, synthesis and characterization is a necessary tool that needs to reach maturity to enable scientific discovery, leading to potential breakthroughs in thermoelectric materials (See Figure 7). The deployment of HT combinatorial methods is expected to lead to an increase in process optimization rate as well as accelerate the discovery of new, non-intuitive materials. Thus, we recommend working towards a closed-loop high-throughput experimentation methodology in order to unravel novel physicochemical phenomena in potential TE material candidates.

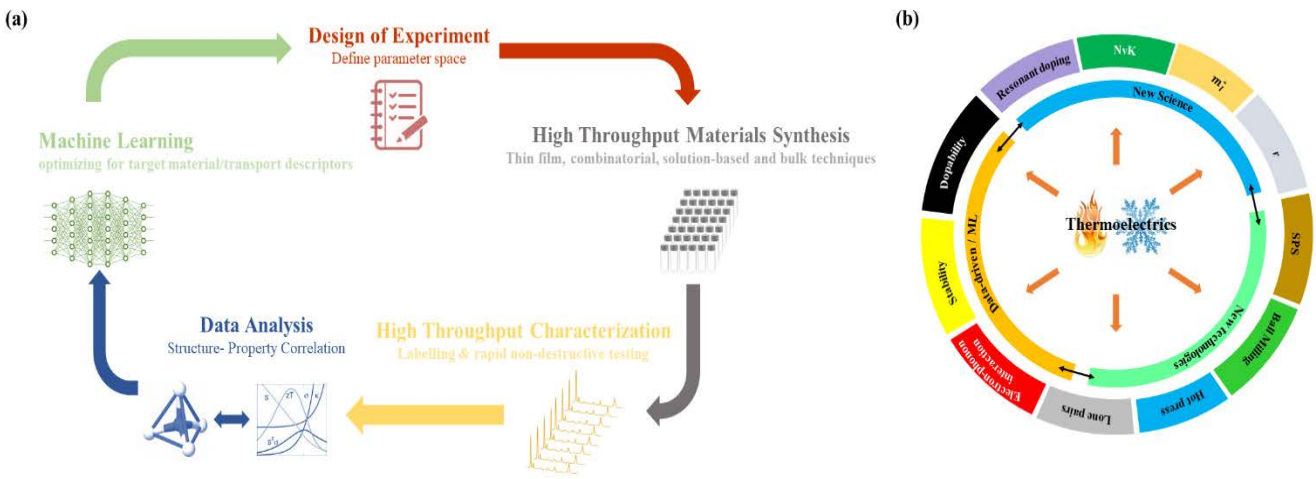

Figure 7. (a) Pictorial representation of a closed-loop workflow for the accelerated discovery of novel materials. (b) All-hierarchical, layered representation of the components that require synergistic tuning for achieving high zT.

In conclusion, we have established the guidelines towards the accelerated discovery of novel TE materials. We revisit both the scientific rationale and the technology employed for the realization of high zT values in case studies of key chalcogenide-based and state-of-the-art thermoelectric materials. We ascertain that the discovery of new TE with high performance is driven by novel scientific phenomena, catalyzed by mature technological processes. To this end, we propose the use of causality-built TE descriptors that can be experimentally measured, combined with closed-loop high-throughput experimentation for the discovery of unexplored, high performing TE materials.

Supporting Information

Supplementary Table 1: List of materials, publication years, temperature of peak zT, scientific and technological ratings, system and colour (for plotting purposes) and references.

References

(1) Bell, L. E. Cooling, Heating, Generating Power, and Recovering Waste Heat with Thermoelectric Systems. *Science* **2008**, *321* (5895), 1457–1461. https://doi.org/10.1126/science.1158899.

(2) Snyder, G. J.; Toberer, E. S. Complex Thermoelectric Materials. *Nat. Mater.* **2008**, *7*

(2), 105–114. https://doi.org/10.1038/nmat2090.

(3) Slack, G. A. The Thermal Conductivity of Nonmetallic Crystals. In *Solid State Physics - Advances in Research and Applications*; 1979; Vol. 34, pp 1–71. https://doi.org/10.1016/S0081-1947(08)60359-8.

(4) Tritt, T. M.; Subramanian, M. a. Thermoelectric Materials, Phenomena, and Applications : A Bird' s Eye View. *MRS Bull.* **2006**, *31* (March), 188–198. https://doi.org/10.1557/mrs2006.44.

(5) Menon, A. K.; Yee, S. K. Design of a Polymer Thermoelectric Generator Using Radial Architecture. *J. Appl. Phys.* **2016**, *119* (5), 055501. https://doi.org/10.1063/1.4941101.

(6) Chowdhury, I.; Prasher, R.; Lofgreen, K.; Chrysler, G.; Narasimhan, S.; Mahajan, R.; Koester, D.; Alley, R.; Venkatasubramanian, R. On-Chip Cooling by Superlattice-Based Thin-Film Thermoelectrics. *Nat. Nanotechnol.* **2009**, *4* (4), 235–238. https://doi.org/10.1038/nnano.2008.417.

(7) Nan, K.; Kang, S. D.; Li, K.; Yu, K. J.; Zhu, F.; Wang, J.; Dunn, A. C.; Zhou, C.; Xie, Z.; Agne, M. T.; Wang, H.; Luan, H.; Zhang, Y.; Huang, Y.; Snyder, G. J.; Rogers, J. A. Compliant and Stretchable Thermoelectric Coils for Energy Harvesting in Miniature Flexible Devices. *Sci. Adv.* **2018**, *4* (11), eaau5849. https://doi.org/10.1126/sciadv.aau5849.

(8) Kittel, C. Interpretation of the Thermal Conductivity of Glasses. *Phys. Rev.* **1949**, *75* (6), 972–974. https://doi.org/10.1103/PhysRev.75.972.

(9) Goldsmid, H. J. *Introduction to Thermoelectricity*; Hull, R., Osgood Jr., R. M., Parisi, J., Warlimont, H., Eds.; Springer Series in Materials Science; Springer Berlin Heidelberg: Berlin, Heidelberg, 2010; Vol. 121. https://doi.org/10.1007/978-3-642-00716-3.

(10) Pei, Y.; Shi, X.; LaLonde, A.; Wang, H.; Chen, L.; Snyder, G. J. Convergence of Electronic Bands for High Performance Bulk Thermoelectrics. *Nature* **2011**, *473* (7345), 66–69. https://doi.org/10.1038/nature09996.

(11) Toberer, E. S.; Zevalkink, A.; Snyder, G. J. Phonon Engineering through Crystal Chemistry. *J. Mater. Chem.* **2011**, *21* (40), 15843–15852. https://doi.org/10.1039/c1jm11754h.

(12) Zevalkink, A.; Smiadak, D. M.; Blackburn, J. L.; Ferguson, A. J.; Chabinyc, M. L.; Delaire, O.; Wang, J.; Kovnir, K.; Martin, J.; Schelhas, L. T.; Sparks, T. D.; Kang, S. D.; Dylla, M. T.; Snyder, G. J.; Ortiz, B. R.; Toberer, E. S. A Practical Field Guide to Thermoelectrics: Fundamentals, Synthesis, and Characterization. *Appl. Phys. Rev.*

2018, *Submitted* (2015). https://doi.org/10.1063/1.5021094.

(13) Lundstrom, M. Carrier Scattering. In *Fundamentals of Carrier Transport*; John Wiley & Sons, Ltd: Chichester, UK, 2006; pp 271–343. https://doi.org/10.1002/0470010827.ch9.

(14) Gibbs, Z. M.; Ricci, F.; Li, G.; Zhu, H.; Persson, K.; Ceder, G.; Hautier, G.; Jain, A.; Snyder, G. J. Effective Mass and Fermi Surface Complexity Factor from Ab Initio Band Structure Calculations. *npj Comput. Mater.* **2017**, *3* (1), 1–6. https://doi.org/10.1038/s41524-017-0013-3.

(15) Witkoske, E.; Wang, X.; Lundstrom, M.; Askarpour, V.; Maassen, J. Thermoelectric Band Engineering: The Role of Carrier Scattering. *J. Appl. Phys.* **2017**, *122* (17), 175102. https://doi.org/10.1063/1.4994696.

(16) Jain, A.; Ong, S. P.; Hautier, G.; Chen, W.; Richards, W. D.; Dacek, S.; Cholia, S.; Gunter, D.; Skinner, D.; Ceder, G.; Persson, K. A. Commentary: The Materials Project: A Materials Genome Approach to Accelerating Materials Innovation. *APL Mater.* **2013**, *1* (1), 011002. https://doi.org/10.1063/1.4812323.

(17) Taylor, R. H.; Rose, F.; Toher, C.; Levy, O.; Yang, K.; Buongiorno Nardelli, M.; Curtarolo, S. A RESTful API for Exchanging Materials Data in the AFLOWLIB.Org Consortium. *Comput. Mater. Sci.* **2014**, *93*, 178–192. https://doi.org/10.1016/j.commatsci.2014.05.014.

(18) Citrine Informatics https://citrination.com. (accessed Oct 30, 2018).

(19) Blaiszik, B.; Chard, K.; Pruyne, J.; Ananthakrishnan, R.; Tuecke, S.; Foster, I. The Materials Data Facility : Data Services to Advance Materials Science Research. *J. Miner. Met. Mateirals Soc.* **2016**, *68* (8), 2045–2052. https://doi.org/10.1007/s11837-016-2001-3.

(20) MPDS https://mpds.io/ (accessed Oct 30, 2018).

(21) Kirklin, S.; Saal, J. E.; Meredig, B.; Thompson, A.; Doak, J. W.; Aykol, M.; Rühl, S.; Wolverton, C. The Open Quantum Materials Database (OQMD): Assessing the Accuracy of DFT Formation Energies. *npj Comput. Mater.* **2015**, *1* (September). https://doi.org/10.1038/npjcompumats.2015.10.

(22) Otsuka, S.; Kuwajima, I.; Hosoya, J.; Xu, Y.; Yamazaki, M. PoLyInfo: Polymer Database for Polymeric Materials Design. In *2011 International Conference on Emerging Intelligent Data and Web Technologies*; IEEE, 2011; pp 22–29. https://doi.org/10.1109/EIDWT.2011.13.

(23) Xi, L.; Pan, S.; Li, X.; Xu, Y.; Ni, J.; Sun, X.; Yang, J.; Luo, J.; Xi, J.; Zhu, W.; Li, X;

Di, J.; Dronskowski R.; Shi, X.; Snyder, G. J.; Zhang, W. Discovery of High-Performance Thermoelectric Chalcogenides through Reliable High-Throughput Material Screening. *J. Am. Chem. Soc.* **2018**, *140* (34), 10785–10793. https://doi.org/10.1021/jacs.8b04704.

(24) Hippalgaonkar, K.; Wang, Y.; Ye, Y.; Qiu, D. Y.; Zhu, H.; Wang, Y.; Moore, J.; Louie, S. G.; Zhang, X. High Thermoelectric Power Factor in Two-Dimensional Crystals of MoS2. *Phys. Rev. B* **2017**, *95* (11), 115407. https://doi.org/10.1103/PhysRevB.95.115407.

(25) Wan, C.; Gu, X.; Dang, F.; Itoh, T.; Wang, Y.; Sasaki, H.; Kondo, M.; Koga, K.; Yabuki, K.; Snyder, G. J.; Yang, R.; Koumoto, K. Flexible N-Type Thermoelectric Materials by Organic Intercalation of Layered Transition Metal Dichalcogenide TiS2. *Nat. Mater.* **2015**, *14* (6), 622–627. https://doi.org/10.1038/nmat4251.

(26) Zhou, J.; Zhu, H.; Liu, T.-H.; Song, Q.; He, R.; Mao, J.; Liu, Z.; Ren, W.; Liao, B.; Singh, D. J.; Ren, Z.; Chen, G. Large Thermoelectric Power Factor from Crystal Symmetry-Protected Non-Bonding Orbital in Half-Heuslers. *Nat. Commun.* **2018**, *9* (1), 1721. https://doi.org/10.1038/s41467-018-03866-w.

(27) Shi, X.; Yang, J.; Salvador, J. R.; Chi, M.; Cho, J. Y.; Wang, H.; Bai, S.; Yang, J.; Zhang, W.; Chen, L. Multiple-Filled Skutterudites: High Thermoelectric Figure of Merit through Separately Optimizing Electrical and Thermal Transports. *J. Am. Chem. Soc.* **2011**, *133* (20), 7837–7846. https://doi.org/10.1021/ja111199y.

(28) Norman, C.; Azough, F.; Freer, R. Chapter 3. Thermoelectric Oxides. In *Thermoelectric Materials and Devices*; Royal Society of Chemistry: Cambridge; pp 60–82. https://doi.org/10.1039/9781782624042-00060.

(29) Sootsman, J. R.; Chung, D. Y.; Kanatzidis, M. G. New and Old Concepts in Thermoelectric Materials. *Angew. Chemie - Int. Ed.* **2009**, *48* (46), 8616–8639. https://doi.org/10.1002/anie.200900598.

(30) Zhang, X.; Pei, Y. Manipulation of Charge Transport in Thermoelectrics. *npj Quantum Mater.* **2017**, *2* (1), 68. https://doi.org/10.1038/s41535-017-0071-2.

(31) Poudel, B.; Hao, Q.; Ma, Y.; Lan, Y.; Minnich, A.; Yu, B.; Yan, X.; Wang, D.; Muto, A.; Vashaee, D.; Chen, X.; Liu, J.; Dresselhaus, M. S.; Chen, G.; Ren, Z. High-Thermoelectric Performance of Nanostructured Bismuth Antimony Telluride Bulk Alloys. *Science* **2008**, *320* (5876), 634–638. https://doi.org/10.1126/science.1156446.

(32) Ong, S. P.; Richards, W. D.; Jain, A.; Hautier, G.; Kocher, M.; Cholia, S.; Gunter, D.; Chevrier, V. L.; Persson, K. A.; Ceder, G. Python Materials Genomics (Pymatgen): A

Robust, Open-Source Python Library for Materials Analysis. *Comput. Mater. Sci.* **2013**, *68*, 314–319. https://doi.org/10.1016/j.commatsci.2012.10.028.

(33) Tshitoyan, V.; Dagdelen, J.; Weston, L.; Dunn, A.; Rong, Z.; Kononova, O.; Persson, K. A.; Ceder, G.; Jain, A. Unsupervised Word Embeddings Capture Latent Knowledge from Materials Science Literature. *Nature* **2019**, *571* (7763), 95–98. https://doi.org/10.1038/s41586-019-1335-8.

(34) Hellenbrandt, M. The Inorganic Crystal Structure Database (ICSD)—Present and Future. *Crystallogr. Rev.* **2004**, *10* (1), 17–22. https://doi.org/10.1080/08893110410001664882.

(35) Yan, J.; Gorai, P.; Ortiz, B.; Miller, S.; Barnett, S. A.; Mason, T.; Stevanović, V.; Toberer, E. S. Material Descriptors for Predicting Thermoelectric Performance. *Energy Environ. Sci.* **2015**, *8* (3), 983–994. https://doi.org/10.1039/C4EE03157A.

(36) Gorai, P.; Gao, D.; Ortiz, B.; Miller, S.; Barnett, S. A.; Mason, T.; Lv, Q.; Stevanović, V.; Toberer, E. S. TE Design Lab: A Virtual Laboratory for Thermoelectric Material Design. *Comput. Mater. Sci.* **2016**, *112*, 368–376. https://doi.org/10.1016/j.commatsci.2015.11.006.

(37) Gaultois, M. W.; Sparks, T. D.; Borg, C. K. H.; Seshadri, R.; Bonificio, W. D.; Clarke, D. R. Data-Driven Review of Thermoelectric Materials: Performance and Resource Considerations. *Chem. Mater.* **2013**, *25* (15), 2911–2920. https://doi.org/10.1021/cm400893e.

(38) Kononova, O.; Huo, H.; He, T.; Rong, Z.; Botari, T.; Sun, W.; Tshitoyan, V.; Ceder, G. Text-Mined Dataset of Inorganic Materials Synthesis Recipes. *Sci. Data* **2019**, *6* (1), 203. https://doi.org/10.1038/s41597-019-0224-1.

(39) Glassbrenner, C. J.; Slack, G. A. Thermal Conductivity of Silicon and Germanium from 3°K to the Melting Point. *Phys. Rev.* **1964**, *134* (4A), A1058–A1069. https://doi.org/10.1103/PhysRev.134.A1058.

(40) Rhyee, J.-S.; Lee, K. H.; Lee, S. M.; Cho, E.; Kim, S. Il; Lee, E.; Kwon, Y. S.; Shim, J. H.; Kotliar, G. Peierls Distortion as a Route to High Thermoelectric Performance in In4Se3-δ Crystals. *Nature* **2009**, *459* (7249), 965–968. https://doi.org/10.1038/nature08088.

(41) Chang, C.; Wu, M.; He, D.; Pei, Y.; Wu, C.-F.; Wu, X.; Yu, H.; Zhu, F.; Wang, K.; Chen, Y.; Huang, L.; Li, J.-F.; He, J.; Zhao, L.-D. 3D Charge and 2D Phonon Transports Leading to High Out-of-Plane ZT in n-Type SnSe Crystals. *Science (80-.).* **2018**, *360* (6390), 778–783. https://doi.org/10.1126/science.aaq1479.

(42) Ortiz, B. R.; Adamczyk, J. M.; Gordiz, K.; Braden, T.; Toberer, E. S. Towards the High-Throughput Synthesis of Bulk Materials: Thermoelectric PbTe–PbSe–SnTe–SnSe Alloys. *Mol. Syst. Des. Eng.* **2019**, *4* (2), 407–420. https://doi.org/10.1039/C8ME00073E.

(43) Correa-Baena, J.-P.; Hippalgaonkar, K.; van Duren, J.; Jaffer, S.; Chandrasekhar, V. R.; Stevanovic, V.; Wadia, C.; Guha, S.; Buonassisi, T. Accelerating Materials Development via Automation, Machine Learning, and High-Performance Computing. *Joule* **2018**, *2* (8), 1410–1420. https://doi.org/10.1016/j.joule.2018.05.009.

(44) Wang H., Pei Y., LaLonde A.D., J. S. G. *Material Design Considerations Based on Thermoelectric Quality Factor*; Koumoto, K., Mori, T., Eds.; Springer Series in Materials Science; Springer Berlin Heidelberg: Berlin, Heidelberg, 2013; Vol. 182. https://doi.org/10.1007/978-3-642-37537-8.

(45) Goldsmid, H. J.; Sharp, J. W. Estimation of the Thermal Band Gap of a Semiconductor from Seebeck Measurements. **1999**, *28* (7), 1–4.

(46) Gibbs, Z. M.; Kim, H.-S.; Wang, H.; Snyder, G. J. Band Gap Estimation from Temperature Dependent Seebeck Measurement—Deviations from the 2e|S|maxTmax Relation. *Appl. Phys. Lett.* **2015**, *106* (2), 022112. https://doi.org/10.1063/1.4905922.

(47) Slack, G. New Materials and Performance Limits for Thermoelectric Cooling. *CRC Handb. Thermoelectr.* **1995**. https://doi.org/10.1201/9781420049718.ch34.

(48) Zeier, W. G.; Zevalkink, A.; Gibbs, Z. M.; Hautier, G.; Kanatzidis, M. G.; Snyder, G. J. Thinking Like a Chemist: Intuition in Thermoelectric Materials. *Angew. Chemie Int. Ed.* **2016**, *55* (24), 6826–6841. https://doi.org/10.1002/anie.201508381.

(49) Chasmar, R. P.; Stratton, R. The Thermoelectric Figure of Merit and Its Relation to Thermoelectric Generators†. *J. Electron. Control* **1959**, *7* (1), 52–72. https://doi.org/10.1080/00207215908937186.

(50) Nolas, G. S.; Sharp, J.; Goldsmid, H. J. *Thermoelectrics Basic Principles and New Materials Developments*; Springer Series in MATERIALS SCIENCE; Springer Berlin Heidelberg: Berlin, Heidelberg, 2001; Vol. 45. https://doi.org/10.1007/978-3-662-04569-5.

(51) Suwardi, A.; Bash, D.; Ng, H. K.; Gomez, J. R.; Repaka, D. V. M.; Kumar, P.; Hippalgaonkar, K. Inertial Effective Mass as an Effective Descriptor for Thermoelectrics via Data-Driven Evaluation. *J. Mater. Chem. A* **2019**, *7* (41), 23762–23769. https://doi.org/10.1039/C9TA05967A.

(52) Parker, D. S.; May, A. F.; Singh, D. J. Benefits of Carrier-Pocket Anisotropy to

Thermoelectric Performance: The Case of p-Type AgBiSe2. *Phys. Rev. Appl.* **2015**, *3* (6), 064003. https://doi.org/10.1103/PhysRevApplied.3.064003.

(53) MacDonald, D. K. C.; Roy, S. K. Vibrational Anharmonicity and Lattice Thermal Properties. II. *Phys. Rev.* **1955**, *97* (3), 673–676. https://doi.org/10.1103/PhysRev.97.673.

(54) Dutta, M.; Pal, K.; Waghmare, U. V.; Biswas, K. Bonding Heterogeneity and Lone Pair Induced Anharmonicity Resulted in Ultralow Thermal Conductivity and Promising Thermoelectric Properties in N-Type AgPbBiSe 3. *Chem. Sci.* **2019**, *10* (18), 4905–4913. https://doi.org/10.1039/C9SC00485H.

(55) Nielsen, M. D.; Ozolins, V.; Heremans, J. P. Lone Pair Electrons Minimize Lattice Thermal Conductivity. *Energy Environ. Sci.* **2013**, *6* (2), 570–578. https://doi.org/10.1039/C2EE23391F.

(56) Xing, G.; Sun, J.; Li, Y.; Fan, X.; Zheng, W.; Singh, D. J. Electronic Fitness Function for Screening Semiconductors as Thermoelectric Materials. *Phys. Rev. Mater.* **2017**, *1* (6), 065405. https://doi.org/10.1103/PhysRevMaterials.1.065405.

(57) Samsonidze, G.; Kozinsky, B. Accelerated Screening of Thermoelectric Materials by First-Principles Computations of Electron-Phonon Scattering. *Adv. Energy Mater.* **2018**, *8* (20), 1800246. https://doi.org/10.1002/aenm.201800246.

(58) Guttmann, Gilad M Gelbstein, Y. Mechanical Properties of Thermoelectric Materials for Practical Applications. In *Bringing Thermoelectricity into Reality*; Aranguren, Y. G. E.-P., Ed.; IntechOpen: Rijeka, 2018; pp 63–80. https://doi.org/10.5772/intechopen.75476.

(59) Yang, J.; Caillat, T. Thermoelectric Materials for Space and Automotive Power Generation. *MRS Bull.* **2006**, *31* (3), 224–229. https://doi.org/10.1557/mrs2006.49.

(60) Maynard, J. Resonant Ultrasound Spectroscopy. *Phys. Today* **1996**, *49* (1), 26.

(61) Zheng, Y.; Tan, X. Y.; Wan, X.; Cheng, X.; Liu, Z.; Yan, Q. Thermal Stability and Mechanical Response of Bi2Te3-Based Materials for Thermoelectric Applications. *ACS Appl. Energy Mater.* **2019**. https://doi.org/10.1021/acsaem.9b02093.

(62) He, R.; Gahlawat, S.; Guo, C.; Chen, S.; Dahal, T.; Zhang, H.; Liu, W.; Zhang, Q.; Chere, E.; White, K.; et al. Studies on Mechanical Properties of Thermoelectric Materials by Nanoindentation. *Phys. status solidi* **2015**, *212* (10), 2191–2195. https://doi.org/10.1002/pssa.201532045.

(63) Li, G.; Aydemir, U.; Morozov, S. I.; Miller, S. A.; An, Q.; Goddard, W. A.; Zhai, P.; Zhang, Q.; Snyder, G. J. Mechanical Properties in Thermoelectric Oxides: Ideal

Strength, Deformation Mechanism, and Fracture Toughness. *Acta Mater.* **2018**, *149*, 341–349. https://doi.org/https://doi.org/10.1016/j.actamat.2018.02.063.

(64) Goldsmid, H. J.; Douglas, R. W. The Use of Semiconductors in Thermoelectric Refrigeration. *Br. J. Appl. Phys.* **1954**, *5* (11), 386–390. https://doi.org/10.1088/0508-3443/5/11/303.

(65) Witting, I. T.; Chasapis, T. C.; Ricci, F.; Peters, M.; Heinz, N. A.; Hautier, G.; Snyder, G. J. The Thermoelectric Properties of Bismuth Telluride. *Adv. Electron. Mater.* **2019**, *5* (6), 1800904. https://doi.org/10.1002/aelm.201800904.

(66) Imamuddin, M.; Dupre, A. Thermoelectric Properties of P-Type Bi2Te3–Sb2Te3–Sb2Se3 Alloys and n-Type Bi2Te3–Bi2Se3 Alloys in the Temperature Range 300 to 600 K. *Phys. status solidi* **1972**, *10* (2), 415–424. https://doi.org/10.1002/pssa.2210100210.

(67) Kim, S. I.; Lee, K. H.; Mun, H. A.; Kim, H. S.; Hwang, S. W.; Roh, J. W.; Yang, D. J.; Shin, W. H.; Li, X. S.; Lee, Y. H.; Snyder, G. J.; Kim. S. W. Dense Dislocation Arrays Embedded in Grain Boundaries for High-Performance Bulk Thermoelectrics. *Science (80-.).* **2015**, *348* (6230), 109–114. https://doi.org/10.1126/science.aaa4166.

(68) Jaworski, C. M.; Kulbachinskii, V.; Heremans, J. P. Resonant Level Formed by Tin in Bi2Te3 and the Enhancement of Room-Temperature Thermoelectric Power. *Phys. Rev. B* **2009**, *80* (23), 233201. https://doi.org/10.1103/PhysRevB.80.233201.

(69) Heremans, J. P. & Wiendlocha, B. in. Tetradymites: Bi2Te3 Related Materials. In *Materials Aspect of Thermoelectricity*; Uher, C., Ed.; CRC Press, 2016; pp 39–94.

(70) Kim, H. S.; Heinz, N. A.; Gibbs, Z. M.; Tang, Y.; Kang, S. D.; Snyder, G. J. High Thermoelectric Performance in (Bi0.25Sb0.75)2Te3 Due to Band Convergence and Improved by Carrier Concentration Control. *Mater. Today* **2017**, *20* (8), 452–459. https://doi.org/10.1016/j.mattod.2017.02.007.

(71) Son, J. H.; Oh, M. W.; Kim, B. S.; Park, S. D.; Min, B. K.; Kim, M. H.; Lee, H. W. Effect of Ball Milling Time on the Thermoelectric Properties of P-Type (Bi,Sb)2Te3. *J. Alloys Compd.* **2013**, *566*, 168–174. https://doi.org/https://doi.org/10.1016/j.jallcom.2013.03.062.

(72) Ravich, Y. I.; Efimova, B. A.; Smirnov, I. A. *Semiconducting Lead Chalcogenides*; Stil'bans, L. S., Ed.; Springer US: Boston, MA, 1970. https://doi.org/10.1007/978-1-4684-8607-0.

(73) *Atomic Power in Space*; Planning & Human Systems, prepared for Department of Energy, USA, 1987.

(74) Heikes, R. *Thermoelectricity: Science and Engineering*; Heikes R. and Ure, R., Ed.; Interscience Publishers: New York, United States.

(75) Ioffe, A. *Semiconductor Thermoelements and Thermoelectric Cooling*; Infosearch: Lodon, 1957.

(76) LaLonde, A. D.; Pei, Y.; Wang, H.; Jeffrey Snyder, G. Lead Telluride Alloy Thermoelectrics. *Mater. Today* **2011**, *14* (11), 526–532. https://doi.org/10.1016/S1369-7021(11)70278-4.

(77) Hicks, L. D.; Dresselhaus, M. S. Thermoelectric Figure of Merit of a One-Dimensional Conductor. *Phys. Rev. B* **1993**, *47* (24), 16631–16634. https://doi.org/10.1103/PhysRevB.47.16631.

(78) Hicks, L. D.; Dresselhaus, M. S. Effect of Quantum-Well Structures on the Thermoelectric Figure of Merit. *Phys. Rev. B* **1993**, *47* (19), 12727–12731. https://doi.org/10.1103/PhysRevB.47.12727.

(79) Heremans, J. P.; Jovovic, V.; Toberer, E. S.; Saramat, A.; Kurosaki, K.; Charoenphakdee, A.; Yamanaka, S.; Snyder, G. J. Enhancement of Thermoelectric Efficiency in PbTe by Distortion of the Electronic Density of States. *Science (80-.).* **2008**, *321* (5888), 554–557. https://doi.org/10.1126/science.1159725.

(80) Hsu, K. F.; Loo, S.; Guo, F.; Chen, W.; Dyck, J. S.; Uher, C.; Hogan, T.; Polychroniadis, E. K.; Kanatzidis, M. G. Cubic AgPbmSbTe2+m: Bulk Thermoelectric Materials with High Figure of Merit. *Science (80-.).* **2004**, *303* (5659), 818 LP – 821. https://doi.org/10.1126/science.1092963.

(81) Biswas, K.; He, J.; Blum, I. D.; Wu, C.-I.; Hogan, T. P.; Seidman, D. N.; Dravid, V. P.; Kanatzidis, M. G. High-Performance Bulk Thermoelectrics with All-Scale Hierarchical Architectures. *Nature* **2012**, *489*, 414.

(82) Chen, L.-C.; Chen, P.-Q.; Li, W.-J.; Zhang, Q.; Struzhkin, V. V.; Goncharov, A. F.; Ren, Z.; Chen, X.-J. Enhancement of Thermoelectric Performance across the Topological Phase Transition in Dense Lead Selenide. *Nat. Mater.* **2019**. https://doi.org/10.1038/s41563-019-0499-9.

(83) Zhou, M.; Gibbs, Z. M.; Wang, H.; Han, Y.; Xin, C.; Li, L.; Snyder, G. J.; Li, J. Q.; Huang, S.; Chen, Z. P.; et al. Optimization of Thermoelectric Efficiency in SnTe: The Case for the Light Band. *Phys. Chem. Chem. Phys.* **2018**, *19* (42), 28749–28755. https://doi.org/10.1002/adfm.201803586.

(84) Tan, G.; Zhao, L.-D.; Shi, F.; Doak, J. W.; Lo, S.-H.; Sun, H.; Wolverton, C.; Dravid, V. P.; Uher, C.; Kanatzidis, M. G. High Thermoelectric Performance of P-Type SnTe

via a Synergistic Band Engineering and Nanostructuring Approach. *J. Am. Chem. Soc.* **2014**, *136* (19), 7006–7017. https://doi.org/10.1021/ja500860m.

(85) Tang, J.; Gao, B.; Lin, S.; Li, J.; Chen, Z.; Xiong, F.; Li, W.; Chen, Y.; Pei, Y. Manipulation of Band Structure and Interstitial Defects for Improving Thermoelectric SnTe. *Adv. Funct. Mater.* **2018**, *28* (34), 1803586. https://doi.org/10.1002/adfm.201803586.

(86) Xiao, Y.; Zhao, L.-D. Charge and Phonon Transport in PbTe-Based Thermoelectric Materials. *npj Quantum Mater.* **2018**, *3* (1), 55. https://doi.org/10.1038/s41535-018-0127-y.

(87) You, L.; Liu, Y.; Li, X.; Nan, P.; Ge, B.; Jiang, Y.; Luo, P.; Pan, S.; Pei, Y.; Zhang, W.; et al. Boosting the Thermoelectric Performance of PbSe through Dynamic Doping and Hierarchical Phonon Scattering. *Energy Environ. Sci.* **2018**, *11* (7), 1848–1858. https://doi.org/10.1039/C8EE00418H.

(88) Boschker, J. E.; Wang, R.; Calarco, R. GeTe: A Simple Compound Blessed with a Plethora of Properties. *CrystEngComm* **2017**, *19* (36), 5324–5335. https://doi.org/10.1039/C7CE01040K.

(89) *CRC Handbook of Thermoelectrics*; Rowe, D., Ed.; CRC Press, 1995. https://doi.org/10.1201/9781420049718.

(90) Hong, M.; Zou, J.; Chen, Z. Thermoelectric GeTe with Diverse Degrees of Freedom Having Secured Superhigh Performance. *Adv. Mater.* **2019**, *31* (14), 1807071. https://doi.org/10.1002/adma.201807071.

(91) Christakudi, T. A.; Plachkova, S. K.; Christakudis, G. C. Thermoelectric Power of (GeTe)1−x(Bi2Te3)x Solid Solutions (0 ≦x ≦ 0.05) in the Temperature Interval 80 to 350 K. *Phys. Status Solidi* **1995**, *147* (1), 211–220. https://doi.org/10.1002/pssa.2211470122.

(92) Lewis, J. E. The Defect Structure of Non-Stoichiometric Germanium Telluride from Magnetic Susceptibility Measurements. *Phys. status solidi* **1970**, *38* (1), 131–140. https://doi.org/10.1002/pssb.19700380110.

(93) Damon, D. H.; Lubell, M. S.; Mazelsky, R. Nature of the Defects in Germanium Telluride. *J. Phys. Chem. Solids* **1967**, *28* (3), 520–522. https://doi.org/10.1016/0022-3697(67)90323-X.

(94) Levin, E. M.; Besser, M. F.; Hanus, R. Electronic and Thermal Transport in GeTe: A Versatile Base for Thermoelectric Materials. *J. Appl. Phys.* **2013**, *114* (8), 083713. https://doi.org/10.1063/1.4819222.

(95) Cook, B. A.; Kramer, M. J.; Wei, X.; Harringa, J. L.; Levin, E. M. Nature of the Cubic to Rhombohedral Structural Transformation in (AgSbTe2)15(GeTe)85 Thermoelectric Material. *J. Appl. Phys.* **2007**, *101* (5), 053715. https://doi.org/10.1063/1.2645675.

(96) Puyet, M.; Lenoir, B.; Dauscher, A.; Pécheur, P.; Bellouard, C.; Tobola, J.; Hejtmanek, J. Electronic, Transport, and Magnetic Properties of CaxCo4Sb12 Partially Filled Skutterudites. *Phys. Rev. B* **2006**, *73* (3), 035126. https://doi.org/10.1103/PhysRevB.73.035126.

(97) Yang, S. H.; Zhu, T. J.; Sun, T.; He, J.; Zhang, S. N.; Zhao, X. B. Nanostructures in High-Performance (GeTe) x (AgSbTe 2) 100− x Thermoelectric Materials. *Nanotechnology* **2008**, *19* (24), 245707. https://doi.org/10.1088/0957-4484/19/24/245707.

(98) Salvador, J. R.; Yang, J.; Shi, X.; Wang, H.; Wereszczak, A. A. Transport and Mechanical Property Evaluation of (AgSbTe)1−x(GeTe)x (X=0.80, 0.82, 0.85, 0.87, 0.90). *J. Solid State Chem.* **2009**, *182* (8), 2088–2095. https://doi.org/10.1016/j.jssc.2009.05.024.

(99) Rosi, F. D.; Dismukes, J. P.; Hockings, E. F. Semiconductor Materials for Thermoelectric Power Generation up to 700 C. *Electr. Eng.* **1960**, *79* (6), 450–459. https://doi.org/10.1109/EE.1960.6432651.

(100) Davidow, J.; Gelbstein, Y. A Comparison Between the Mechanical and Thermoelectric Properties of Three Highly Efficient P-Type GeTe-Rich Compositions: TAGS-80, TAGS-85, and 3% Bi2Te3-Doped Ge0.87Pb0.13Te. *J. Electron. Mater.* **2013**, *42* (7), 1542–1549. https://doi.org/10.1007/s11664-012-2316-y.

(101) Chen, Y.; Jaworski, C. M.; Gao, Y. B.; Wang, H.; Zhu, T. J.; Snyder, G. J.; Heremans, J. P.; Zhao, X. B. Transport Properties and Valence Band Feature of High-Performance (GeTe) 85 (AgSbTe 2) 15 Thermoelectric Materials. *New J. Phys.* **2014**, *16* (1), 013057. https://doi.org/10.1088/1367-2630/16/1/013057.

(102) Lee, J. K.; Oh, M. W.; Kim, B. S.; Min, B. K.; Lee, H. W.; Park, S. D. Influence of Mn on Crystal Structure and Thermoelectric Properties of GeTe Compounds. *Electron. Mater. Lett.* **2014**, *10* (4), 813–817. https://doi.org/10.1007/s13391-014-4149-8.

(103) Dado, B.; Gelbstein, Y.; Mogilansky, D.; Ezersky, V.; Dariel, M. P. Structural Evolution Following Spinodal Decomposition of the Pseudoternary Compound (Pb0.3Sn0.1Ge0.6)Te. *J. Electron. Mater.* **2010**, *39* (9), 2165–2171. https://doi.org/10.1007/s11664-009-0980-3.

(104) Gelbstein, Y.; Dado, B.; Ben-Yehuda, O.; Sadia, Y.; Dashevsky, Z.; Dariel, M. P.

Highly Efficient Ge-Rich Ge x Pb1−x Te Thermoelectric Alloys. *J. Electron. Mater.* **2010**, *39* (9), 2049–2052. https://doi.org/10.1007/s11664-009-1012-z.

(105) Li, S. P.; Li, J. Q.; Wang, Q. B.; Wang, L.; Liu, F. S.; Ao, W. Q. Synthesis and Thermoelectric Properties of the (GeTe)1-x(PbTe)x Alloys. *Solid State Sci.* **2011**, *13* (2), 399–403. https://doi.org/10.1016/j.solidstatesciences.2010.11.045.

(106) Plachkovka, S. K.; Georgiev, T. I. Thermoelectric Power of Some Compositions of GeTe-Rich (GeTe) 1-x (AgBiTe 2) x Solid Solutions. *J. Phys. Condens. Matter* **1993**, *5* (1), 67–84. https://doi.org/10.1088/0953-8984/5/1/008.

(107) Zhang, L.; Wang, W.; Ren, B.; Guo, J. The Effect of Adding Nano-Bi2Te3 on Properties of GeTe-Based Thermoelectric Material. *J. Electron. Mater.* **2013**, *42* (7), 1303–1306. https://doi.org/10.1007/s11664-012-2416-8.

(108) Sun, H.; Lu, X.; Chi, H.; Morelli, D. T.; Uher, C. Highly Efficient (In 2 Te 3) x (GeTe) 3−3x Thermoelectric Materials: A Substitute for TAGS. *Phys. Chem. Chem. Phys.* **2014**, *16* (29), 15570–15575. https://doi.org/10.1039/C4CP01294A.

(109) Koenig, J.; Winkler, M.; Dankwort, T.; Hansen, A.-L.; Pernau, H.-F.; Duppel, V.; Jaegle, M.; Bartholomé, K.; Kienle, L.; Bensch, W. Thermoelectric Efficiency of (1 − x)(GeTe) x(Bi 2 Se 0.2 Te 2.8) and Implementation into Highly Performing Thermoelectric Power Generators. *Dalt. Trans.* **2015**, *44* (6), 2835–2843. https://doi.org/10.1039/C4DT03425B.

(110) Rosenthal, T.; Schneider, M. N.; Stiewe, C.; Döblinger, M.; Oeckler, O. Real Structure and Thermoelectric Properties of GeTe-Rich Germanium Antimony Tellurides. *Chem. Mater.* **2011**, *23* (19), 4349–4356. https://doi.org/10.1021/cm201717z.

(111) Perumal, S.; Roychowdhury, S.; Negi, D. S.; Datta, R.; Biswas, K. High Thermoelectric Performance and Enhanced Mechanical Stability of p -Type Ge 1– x Sb x Te. *Chem. Mater.* **2015**, *27* (20), 7171–7178. https://doi.org/10.1021/acs.chemmater.5b03434.

(112) Perumal, S.; Roychowdhury, S.; Biswas, K. Reduction of Thermal Conductivity through Nanostructuring Enhances the Thermoelectric Figure of Merit in Ge 1−x Bi x Te. *Inorg. Chem. Front.* **2016**, *3* (1), 125–132. https://doi.org/10.1039/C5QI00230C.

(113) Levin, E. M.; Bud'ko, S. L.; Schmidt-Rohr, K. Enhancement of Thermopower of TAGS-85 High-Performance Thermoelectric Material by Doping with the Rare Earth Dy. *Adv. Funct. Mater.* **2012**, *22* (13), 2766–2774. https://doi.org/10.1002/adfm.201103049.

(114) Levin, E. M.; Cook, B. A.; Harringa, J. L.; Bud'ko, S. L.; Venkatasubramanian, R.;

Schmidt-Rohr, K. Analysis of Ce- and Yb-Doped TAGS-85 Materials with Enhanced Thermoelectric Figure of Merit. *Adv. Funct. Mater.* **2011**, *21* (3), 441–447. https://doi.org/10.1002/adfm.201001307.

(115) Wu, D.; Zhao, L.-D.; Hao, S.; Jiang, Q.; Zheng, F.; Doak, J. W.; Wu, H.; Chi, H.; Gelbstein, Y.; Uher, C.; et al. Origin of the High Performance in GeTe-Based Thermoelectric Materials upon Bi 2 Te 3 Doping. *J. Am. Chem. Soc.* **2014**, *136* (32), 11412–11419. https://doi.org/10.1021/ja504896a.

(116) Li, J.; Zhang, X.; Chen, Z.; Lin, S.; Li, W.; Shen, J.; Witting, I. T.; Faghaninia, A.; Chen, Y.; Jain, A.; et al. Low-Symmetry Rhombohedral GeTe Thermoelectrics. *Joule* **2018**, 1–12. https://doi.org/10.1016/j.joule.2018.02.016.

(117) Zhang, X.; Li, J.; Wang, X.; Chen, Z.; Mao, J.; Chen, Y.; Pei, Y. Vacancy Manipulation for Thermoelectric Enhancements in GeTe Alloys. *J. Am. Chem. Soc.* **2018**, *140* (46), 15883–15888. https://doi.org/10.1021/jacs.8b09375.

(118) Shuai, J.; Tan, X. J.; Guo, Q.; Xu, J. T.; Gellé, A.; Gautier, R.; Halet, J.-F.; Failamani, F.; Jiang, J.; Mori, T. Enhanced Thermoelectric Performance through Crystal Field Engineering in Transition Metal–Doped GeTe. *Mater. Today Phys.* **2019**, *9*, 100094. https://doi.org/10.1016/j.mtphys.2019.100094.

(119) Banik, A.; Ghosh, T.; Arora, R.; Dutta, M.; Pandey, J.; Acharya, S.; Soni, A.; Waghmare, U. V.; Biswas, K. Engineering Ferroelectric Instability to Achieve Ultralow Thermal Conductivity and High Thermoelectric Performance in Sn 1−x Ge x Te. *Energy Environ. Sci.* **2019**, *12* (2), 589–595. https://doi.org/10.1039/C8EE03162B.

(120) Liu, R.; Chen, H.; Zhao, K.; Qin, Y.; Jiang, B.; Zhang, T.; Sha, G.; Shi, X.; Uher, C.; Zhang, W.; et al. Entropy as a Gene-Like Performance Indicator Promoting Thermoelectric Materials. *Adv. Mater.* **2017**, *29* (38), 1702712. https://doi.org/10.1002/adma.201702712.

(121) Qiu, Y.; Jin, Y.; Wang, D.; Guan, M.; He, W.; Peng, S.; Liu, R.; Gao, X.; Zhao, L.-D. Realizing High Thermoelectric Performance in GeTe through Decreasing the Phase Transition Temperature via Entropy Engineering. *J. Mater. Chem. A* **2019**. https://doi.org/10.1039/C9TA10963C.

(122) Perumal, S.; Samanta, M.; Ghosh, T.; Shenoy, U. S.; Bohra, A. K.; Bhattacharya, S.; Singh, A.; Waghmare, U. V.; Biswas, K. Realization of High Thermoelectric Figure of Merit in GeTe by Complementary Co-Doping of Bi and In. *Joule* **2019**, *3* (10), 2565–2580. https://doi.org/10.1016/j.joule.2019.08.017.

(123) Nozariasbmarz, A.; Agarwal, A.; Coutant, Z. A.; Hall, M. J.; Liu, J.; Liu, R.; Malhotra,

A.; Norouzzadeh, P.; Öztürk, M. C.; Ramesh, V. P.; et al. Thermoelectric Silicides: A Review. *Jpn. J. Appl. Phys.* **2017**, *56* (5S1), 05DA04. https://doi.org/10.7567/JJAP.56.05DA04.

(124) Basu, R.; Bhattacharya, S.; Bhatt, R.; Roy, M.; Ahmad, S.; Singh, A.; Navaneethan, M.; Hayakawa, Y.; Aswal, D. K.; Gupta, S. K. Improved Thermoelectric Performance of Hot Pressed Nanostructured N-Type SiGe Bulk Alloys. *J. Mater. Chem. A* **2014**, *2* (19), 6922. https://doi.org/10.1039/c3ta14259k.

(125) *Thermoelectrics Handbook*; Rowe, D., Ed.; CRC Press, 2005. https://doi.org/10.1201/9781420038903.

(126) Rosi, F. D. Thermoelectricity and Thermoelectric Power Generation. *Solid. State. Electron.* **1968**, *11* (9), 833–868. https://doi.org/10.1016/0038-1101(68)90104-4.

(127) Slack, G. A.; Hussain, M. A. The Maximum Possible Conversion Efficiency of Silicon-germanium Thermoelectric Generators. *J. Appl. Phys.* **1991**, *70* (5), 2694–2718. https://doi.org/10.1063/1.349385.

(128) Pisharody, R. K.; Garvey, L. P. Modified Silicon-Germanium Alloys with Improved Performance. In *Intersociety Energy Conversion Engineering Conference*; San Diego, 1978; pp 1963–1968.

(129) Kasper, E.; Herzog, H. J.; Kibbel, H. A One-Dimensional SiGe Superlattice Grown by UHV Epitaxy. *Appl. Phys.* **1975**, *8* (3), 199–205. https://doi.org/10.1007/BF00896611.

(130) Joshi, G.; Lee, H.; Lan, Y.; Wang, X.; Zhu, G.; Wang, D.; Gould, R. W.; Cuff, D. C.; Tang, M. Y.; Dresselhaus, M. S.; Chen, G.; Ren, Z. Enhanced Thermoelectric Figure-of-Merit in Nanostructured p-Type Silicon Germanium Bulk Alloys. *Nano Lett.* **2008**, *8* (12), 4670–4674. https://doi.org/10.1021/nl8026795.

(131) Wang, X. W.; Lee, H.; Lan, Y. C.; Zhu, G. H.; Joshi, G.; Wang, D. Z.; Yang, J.; Muto, A. J.; Tang, M. Y.; Klatsky, J.; et al. Enhanced Thermoelectric Figure of Merit in Nanostructured N-Type Silicon Germanium Bulk Alloy. *Appl. Phys. Lett.* **2008**, *93* (19), 193121. https://doi.org/10.1063/1.3027060.

(132) Yu, B.; Zebarjadi, M.; Wang, H.; Lukas, K.; Wang, H.; Wang, D.; Opeil, C.; Dresselhaus, M.; Chen, G.; Ren, Z. Enhancement of Thermoelectric Properties by Modulation-Doping in Silicon Germanium Alloy Nanocomposites. *Nano Lett.* **2012**, *12* (4), 2077–2082. https://doi.org/10.1021/nl3003045.

(133) Zhao, L.-D.; Chang, C.; Tan, G.; Kanatzidis, M. G. SnSe: A Remarkable New Thermoelectric Material. *Energy Environ. Sci.* **2016**, *9* (10), 3044–3060. https://doi.org/10.1039/C6EE01755J.

(134) Shi, W.; Gao, M.; Wei, J.; Gao, J.; Fan, C.; Ashalley, E.; Li, H.; Wang, Z. Tin Selenide (SnSe): Growth, Properties, and Applications. *Adv. Sci.* **2018**, *5* (4), 1700602. https://doi.org/10.1002/advs.201700602.

(135) Albers, W.; Haas, C.; Ober, H.; Schodder, G. R.; Wasscher, J. D. Preparation and Properties of Mixed Crystals SnS(1−x)Sex. *J. Phys. Chem. Solids* **1962**, *23* (3), 215–220. https://doi.org/10.1016/0022-3697(62)90004-5.

(136) Wasscher, J. D.; Albers, W.; Haas, C. Simple Evaluation of the Maximum Thermoelectric Figure of Merit, with Application to Mixed Crystals SnS1-XSex. *Solid. State. Electron.* **1963**, *6* (3), 261–264. https://doi.org/10.1016/0038-1101(63)90083-2.

(137) Zhao, L.-D.; Lo, S.-H.; Zhang, Y.; Sun, H.; Tan, G.; Uher, C.; Wolverton, C.; Dravid, V. P.; Kanatzidis, M. G. Ultralow Thermal Conductivity and High Thermoelectric Figure of Merit in SnSe Crystals. *Nature* **2014**, *508* (7496), 373–377. https://doi.org/10.1038/nature13184.

(138) Zhao, L.-D.; Tan, G.; Hao, S.; He, J.; Pei, Y.; Chi, H.; Wang, H.; Gong, S.; Xu, H.; Dravid, V. P.; et al. Ultrahigh Power Factor and Thermoelectric Performance in Hole-Doped Single-Crystal SnSe. *Science (80-.).* **2016**, *351* (6269), 141–144. https://doi.org/10.1126/science.aad3749.

(139) Chen, C.-L.; Wang, H.; Chen, Y.-Y.; Day, T.; Snyder, G. J. Thermoelectric Properties of P-Type Polycrystalline SnSe Doped with Ag. *J. Mater. Chem. A* **2014**, *2* (29), 11171–11176. https://doi.org/10.1039/C4TA01643B.

(140) Duong, A. T.; Nguyen, V. Q.; Duvjir, G.; Duong, V. T.; Kwon, S.; Song, J. Y.; Lee, J. K.; Lee, J. E.; Park, S.; Min, T.; Lee, J.; Kim, J.; Cho, S. Achieving ZT=2.2 with Bi-Doped n-Type SnSe Single Crystals. *Nat. Commun.* **2016**, *7* (1), 13713. https://doi.org/10.1038/ncomms13713.

(141) Lee, Y. K.; Luo, Z.; Cho, S. P.; Kanatzidis, M. G.; Chung, I. Surface Oxide Removal for Polycrystalline SnSe Reveals Near-Single-Crystal Thermoelectric Performance. *Joule* **2019**, *3* (3), 719–731. https://doi.org/10.1016/j.joule.2019.01.001.

(142) He, W.; Wang, D.; Wu, H.; Xiao, Y.; Zhang, Y.; He, D.; Feng, Y.; Hao, Y.-J.; Dong, J.-F.; Chetty, R.; et al. High Thermoelectric Performance in Low-Cost SnS 0.91 Se 0.09 Crystals. *Science (80-.).* **2019**, *365* (6460), 1418–1424. https://doi.org/10.1126/science.aax5123.

(143) Zhang, J.; Song, L.; Iversen, B. B. Insights into the Design of Thermoelectric Mg3Sb2 and Its Analogs by Combining Theory and Experiment. *npj Comput. Mater.* **2019**, *5* (1), 76. https://doi.org/10.1038/s41524-019-0215-y.

(144) Glatz, W.; Durrer, L.; Schwyter, E.; Hierold, C. Novel Mixed Method for the Electrochemical Deposition of Thick Layers of Bi2+xTe3-Xwith Controlled Stoichiometry. *Electrochim. Acta* **2008**, *54* (2), 755–762. https://doi.org/10.1016/j.electacta.2008.06.065.

(145) Kuo, J. J.; Yu, Y.; Kang, S. D.; Cojocaru-Mirédin, O.; Wuttig, M.; Snyder, G. J. Mg Deficiency in Grain Boundaries of N-Type Mg 3 Sb 2 Identified by Atom Probe Tomography. *Adv. Mater. Interfaces* **2019**, *6* (13), 1900429. https://doi.org/10.1002/admi.201900429.

(146) Shi, X.; Sun, C.; Zhang, X.; Chen, Z.; Lin, S.; Li, W.; Pei, Y. Efficient Sc-Doped Mg 3.05– x Sc x SbBi Thermoelectrics Near Room Temperature. *Chem. Mater.* **2019**, acs.chemmater.9b03156. https://doi.org/10.1021/acs.chemmater.9b03156.

(147) Ohno, S.; Imasato, K.; Anand, S.; Tamaki, H.; Kang, S. D.; Gorai, P.; Sato, H. K.; Toberer, E. S.; Kanno, T.; Snyder, G. J. Phase Boundary Mapping to Obtain N-Type Mg3Sb2-Based Thermoelectrics. *Joule* **2018**, *2* (1), 141–154. https://doi.org/10.1016/j.joule.2017.11.005.

(148) Shi, X.; Sun, C.; Bu, Z.; Zhang, X.; Wu, Y.; Lin, S.; Li, W.; Faghaninia, A.; Jain, A.; Pei, Y. Revelation of Inherently High Mobility Enables Mg 3 Sb 2 as a Sustainable Alternative to N-Bi 2 Te 3 Thermoelectrics. *Adv. Sci.* **2019**, *6* (16), 1802286. https://doi.org/10.1002/advs.201802286.

(149) Imasato, K.; Kang, S. D.; Snyder, G. J. Exceptional Thermoelectric Performance in Mg 3 Sb 0.6 Bi 1.4 for Low-Grade Waste Heat Recovery. *Energy Environ. Sci.* **2019**, *12* (3), 965–971. https://doi.org/10.1039/C8EE03374A.

(150) Mao, J.; Zhu, H.; Ding, Z.; Liu, Z.; Gamage, G. A.; Chen, G.; Ren, Z. High Thermoelectric Cooling Performance of N-Type Mg 3 Bi 2 -Based Materials. *Science (80-.).* **2019**, *365* (6452), 495–498. https://doi.org/10.1126/science.aax7792.

(151) Li, G.; Garcia Fernandez, J.; Lara Ramos, D. A.; Barati, V.; Pérez, N.; Soldatov, I.; Reith, H.; Schierning, G.; Nielsch, K. Integrated Microthermoelectric Coolers with Rapid Response Time and High Device Reliability. *Nat. Electron.* **2018**, *1* (10), 555–561. https://doi.org/10.1038/s41928-018-0148-3.

(152) Hu, G.; Edwards, H.; Lee, M. Silicon Integrated Circuit Thermoelectric Generators with a High Specific Power Generation Capacity. *Nat. Electron.* **2019**, *2* (7), 300–306. https://doi.org/10.1038/s41928-019-0271-9.

(153) Burton, M. R.; Mehraban, S.; Beynon, D.; McGettrick, J.; Watson, T.; Lavery, N. P.; Carnie, M. J. 3D Printed SnSe Thermoelectric Generators with High Figure of Merit.

Adv. Energy Mater. **2019**, *9* (26), 1900201. https://doi.org/10.1002/aenm.201900201.

(154) Brandt, R. E.; Rachel C. Kurchin, Vera Steinmann, Daniil Kitchaev, C. R.; Sergiu Levcenco, Gerbrand Ceder, Thomas Unold, and T. B. Rapid Photovoltaic Device Characterization through Bayesian Parameter Estimation. *Joule* **2017**, *1*, 843–856.

(155) Zhang, J.; Song, L.; Pedersen, S. H.; Yin, H.; Hung, L. T.; Iversen, B. B. Discovery of High-Performance Low-Cost n-Type Mg3Sb2-Based Thermoelectric Materials with Multi-Valley Conduction Bands. *Nat. Commun.* **2017**, *8* (1), 13901. https://doi.org/10.1038/ncomms13901.

(156) Ricci, F.; Chen, W.; Aydemir, U.; Snyder, J.; Rignanese, G.; Jain, A.; Hautier, G. An Ab Initio Electronic Transport Database for Inorganic Materials. *Sci. Data* **2017**, *4*, 170085. https://doi.org/doi:10.5061/dryad.gn001.

(157) Chen, W.; Pöhls, J.-H.; Hautier, G.; Broberg, D.; Bajaj, S.; Aydemir, U.; Gibbs, Z. M.; Zhu, H.; Asta, M.; Snyder, G. J.; et al. Understanding Thermoelectric Properties from High-Throughput Calculations: Trends, Insights, and Comparisons with Experiment. *J. Mater. Chem. C* **2016**, *4* (20), 4414–4426. https://doi.org/10.1039/C5TC04339E.

(158) Isaacs, E. B.; Wolverton, C. Inverse Band Structure Design via Materials Database Screening: Application to Square Planar Thermoelectrics. *Chem. Mater.* **2018**, *30* (5), 1540–1546. https://doi.org/10.1021/acs.chemmater.7b04496.

(159) Davies, D. W.; Butler, K. T.; Jackson, A. J.; Morris, A.; Frost, J. M.; Skelton, J. M.; Walsh, A. Computational Screening of All Stoichiometric Inorganic Materials. *Chem* **2016**, *1* (4), 617–627. https://doi.org/10.1016/j.chempr.2016.09.010.

(160) Urban, J. J.; Menon, A. K.; Tian, Z.; Jain, A.; Hippalgaonkar, K. New Horizons in Thermoelectric Materials: Correlated Electrons, Organic Transport, Machine Learning, and More. *J. Appl. Phys.* **2019**, *125* (18). https://doi.org/10.1063/1.5092525.

(161) Jha, D.; Ward, L.; Paul, A.; Liao, W.; Choudhary, A.; Wolverton, C.; Agrawal, A. ElemNet: Deep Learning the Chemistry of Materials From Only Elemental Composition. *Sci. Rep.* **2018**, *8* (1), 17593. https://doi.org/10.1038/s41598-018-35934-y.

(162) Ye, W.; Chen, C.; Wang, Z.; Chu, I. H.; Ong, S. P. Deep Neural Networks for Accurate Predictions of Crystal Stability. *Nat. Commun.* **2018**, *9* (1), 1–6. https://doi.org/10.1038/s41467-018-06322-x.

(163) Chen, C.; Ye, W.; Zuo, Y.; Zheng, C.; Ong, S. P. Graph Networks as a Universal Machine Learning Framework for Molecules and Crystals. *Chem. Mater.* **2019**, *31* (9), 3564–3572. https://doi.org/10.1021/acs.chemmater.9b01294.

(164) Minggang Zeng, Jatin Nitin Kumar, Zeng Zeng, Ramasamy Savitha, Vijay Ramaseshan Chandrasekhar, and K. H. Graph Convolutional Neural Networks for Polymers Property Prediction. *arXiv* **2018**. https://doi.org/arXiv:1811.06231.

(165) Furmanchuk, A.; Saal, J. E.; Doak, J. W.; Olson, G. B.; Choudhary, A.; Agrawal, A. Prediction of Seebeck Coefficient for Compounds without Restriction to Fixed Stoichiometry: A Machine Learning Approach. *J. Comput. Chem.* **2018**, *39* (4), 191–202. https://doi.org/10.1002/jcc.25067.

(166) Chirag Agarwal, Dan Schonfeld, A. N. Removing Input Features via a Generative Model to Explain Their Attributions to an Image Classifier's Decisions. *arXiv:1910.04256*. https://doi.org/arXiv:1910.04256.

(167) Gromski, P. S.; Granda, J. M.; Cronin, L. Universal Chemical Synthesis and Discovery with 'The Chemputer.' *Trends Chem.* **2019**, *xx* (xx), 1–9. https://doi.org/10.1016/j.trechm.2019.07.004.

(168) MacLeod, B. P.; Parlane, F. G. L.; Morrissey, T. D.; Häse, F.; Roch, L. M.; Dettelbach, K. E.; Moreira, R.; Yunker, L. P. E.; Rooney, M. B.; Deeth, J. R.; et al. Self-Driving Laboratory for Accelerated Discovery of Thin-Film Materials. **2019**.

(169) Kumar, J. N.; Li, Q.; Tang, K. Y. T.; Buonassisi, T.; Gonzalez-Oyarce, A. L.; Ye, J. Machine Learning Enables Polymer Cloud-Point Engineering via Inverse Design. *npj Comput. Mater.* **2019**, *5* (1), 73. https://doi.org/10.1038/s41524-019-0209-9.

(170) Gómez-Bombarelli, R.; Aguilera-Iparraguirre, J.; Hirzel, T. D.; Duvenaud, D.; Maclaurin, D.; Blood-Forsythe, M. A.; Chae, H. S.; Einzinger, M.; Ha, D.-G.; Wu, T.; et al. Design of Efficient Molecular Organic Light-Emitting Diodes by a High-Throughput Virtual Screening and Experimental Approach. *Nat. Mater.* **2016**, *15* (10), 1120–1127. https://doi.org/10.1038/nmat4717.

(171) De Luna, P.; Wei, J.; Bengio, Y.; Aspuru-Guzik, A.; Sargent, E. Use Machine Learning to Find Energy Materials. *Nature* **2017**, *552* (7683), 23–27. https://doi.org/10.1038/d41586-017-07820-6.

(172) Tabor, D. P.; Roch, L. M.; Saikin, S. K.; Kreisbeck, C.; Sheberla, D.; Montoya, J. H.; Dwaraknath, S.; Aykol, M.; Ortiz, C.; Tribukait, H.; et al. Accelerating the Discovery of Materials for Clean Energy in the Era of Smart Automation. *Nat. Rev. Mater.* **2018**, *3* (5), 5–20. https://doi.org/10.1038/s41578-018-0005-z.

(173) Butler, K. T.; Davies, D. W.; Cartwright, H.; Isayev, O.; Walsh, A. Machine Learning for Molecular and Materials Science. *Nature* **2018**, *559* (7715), 547–555. https://doi.org/10.1038/s41586-018-0337-2.

(174) Koinuma, H.; Takeuchi, I. Combinatorial Solid-State Chemistry of Inorganic Materials. *Nat. Mater.* **2004**, *3* (7), 429–438. https://doi.org/10.1038/nmat1157.

(175) Xiang, X.-D.; Sun, X.; Briceno, G.; Lou, Y.; Wang, K.; Chang, H.; Wallace-Freedman, W. G.; Chen, S.-W.; Schultz, P. G. A Combinatorial Approach to Materials Discovery. *Science (80-.).* **1995**, *268* (5218), 1738–1740. https://doi.org/10.1126/science.268.5218.1738.

(176) van Dover, R. B.; Schneemeyer, L. F.; Fleming, R. M. Discovery of a Useful Thin-Film Dielectric Using a Composition-Spread Approach. *Nature* **1998**, *392* (6672), 162–164. https://doi.org/10.1038/32381.

(177) Chang, H.; Takeuchi, I.; Xiang, X. D. A Low-Loss Composition Region Identified from a Thin-Film Composition Spread of (Ba1-x-YSrxCay)TiO3. *Appl. Phys. Lett.* **1999**, *74* (8), 1165–1167. https://doi.org/10.1063/1.123475.

(178) Takeuchi, I.; Lauterbach, J.; Fasolka, M. J. Combinatorial Materials Synthesis. *Mater. Today* **2005**, *8* (10), 18–26. https://doi.org/10.1016/S1369-7021(05)71121-4.

(179) Danielson, E.; Golden, J. H.; McFarland, E. W.; Reaves, C. M.; Weinberg, W. H.; Wu, X. Di. A Combinatorial Approach to the Discovery and Optimization of Luminescent Materials. *Nature* **1997**, *389* (6654), 944–948. https://doi.org/10.1038/40099.

(180) Mao, S. S. High Throughput Combinatorial Screening of Semiconductor Materials. *Appl. Phys. A* **2011**, *105* (2), 283–288. https://doi.org/10.1007/s00339-011-6614-7.

(181) Shinde, S. R.; Ogale, S. B.; Higgins, J. S.; Zheng, H.; Millis, A. J.; Kulkarni, V. N.; Ramesh, R.; Greene, R. L.; Venkatesan, T. Co-Occurrence of Superparamagnetism and Anomalous Hall Effect in Highly Reduced Cobalt-Doped Rutile TiO2−δ Films. *Phys. Rev. Lett.* **2004**, *92* (16), 166601. https://doi.org/10.1103/PhysRevLett.92.166601.

(182) Darr, J. A.; Zhang, J.; Makwana, N. M.; Weng, X. Continuous Hydrothermal Synthesis of Inorganic Nanoparticles: Applications and Future Directions. *Chem. Rev.* **2017**, *117* (17), 11125–11238. https://doi.org/10.1021/acs.chemrev.6b00417.

(183) Howard, D. P.; Marchand, P.; McCafferty, L.; Carmalt, C. J.; Parkin, I. P.; Darr, J. A. High-Throughput Continuous Hydrothermal Synthesis of Transparent Conducting Aluminum and Gallium Co-Doped Zinc Oxides. *ACS Comb. Sci.* **2017**, *19* (4), 239–245. https://doi.org/10.1021/acscombsci.6b00118.

(184) Kremsner, J. M.; Stadler, A.; Kappe, C. O. High-Throughput Microwave-Assisted Organic Synthesis: Moving from Automated Sequential to Parallel Library-Generation Formats in Silicon Carbide Microtiter Plates. *J. Comb. Chem.* **2007**, *9* (2), 285–291.

https://doi.org/10.1021/cc060138z.

(185) Adamczyk, J. M.; Ghosh, S.; Braden, T. L.; Hogan, C. J.; Toberer, E. S. Alloyed Thermoelectric PbTe–SnTe Films Formed via Aerosol Deposition. *ACS Comb. Sci.* **2019**, acscombsci.9b00145. https://doi.org/10.1021/acscombsci.9b00145.

TOC

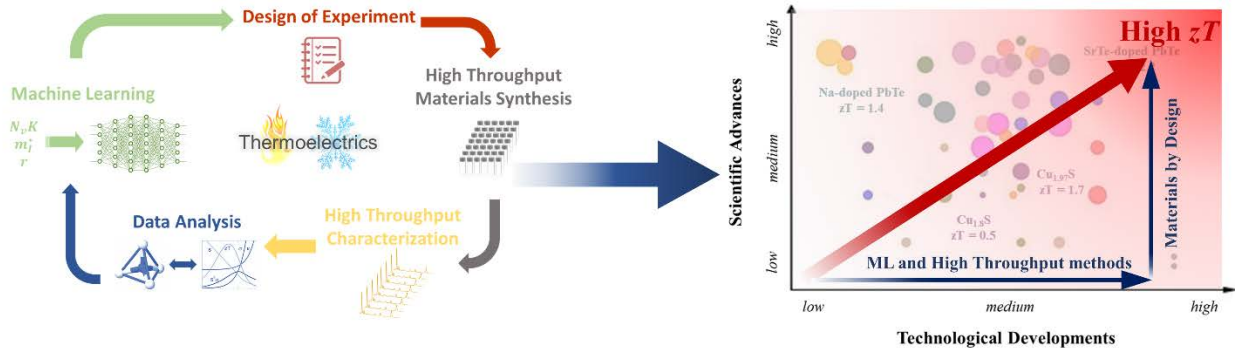
Design of Experiment
Machine Learning
High Throughput
Materials Synthesis
Thermoelectrics
Data Analysis
High Throughput
Characterization
Scientific Advances
high
medium
low
High zT
SrTe-doped PbTe
Na-doped PbTe
zT = 1.4
Cu1.97S
zT = 1.7
Cu1.8S
zT = 0.5
ML and High Throughput methods
Materials by Design
low
medium
high
Technological Developments